

1 Highlights

2 1. Stepwise including topography ~~&and~~ vegetation improved runoff ~~&and~~  
3 snow simulations.

4 ~~Simulations:~~

5 2. ~~Snowmelt contributed 23.5% & 14.7%~~ The ratio of snowmelt runoff to  
6 streamflow was 23.6% and 15.9% in two Mongolian basins.

7 3. High elevations showed slower snowmelt release; low elevations  
8 ~~responded rapidly to generate rapid, rainfall-events-driven runoff.~~

9

10

11

12

13

14

15

16

17

18

19

20

21

22

23

24 **Revealing the Influence of Topography and Vegetation on**  
25 **Hydrological Processes Using a Stepwise Modelling Approach in Cold**  
26 **Alpine Basins of the Mongolian Plateau**

27 Leilei Yong <sup>1</sup>, Yahui Wang <sup>1</sup>, Batsuren Dorjsuren <sup>2</sup>, Zheng Duan <sup>3</sup>, Hongkai  
28 Gao <sup>1\*</sup>

29 <sup>1</sup> Key Laboratory of Geographic Information Science (Ministry of  
30 Education of China), School of Geographical Sciences, East China Normal  
31 University, Shanghai, China

32 <sup>2</sup> Department of Environment and Forest Engineering, National University  
33 of Mongolia, Ulaanbaatar 210646, Mongolia

34 <sup>3</sup> Department of Physical Geography and Ecosystem Science, Lund  
35 University, Sölvegatan 12, SE-223 62, Lund, Sweden

36

37 \* Correspondence: Hongkai Gao,

38 [hkgao@geo.ecnu.edu.cn](mailto:hkgao@geo.ecnu.edu.cn)  
~~[hkgao@geo.ecnu.edu.cn](mailto:hkgao@geo.ecnu.edu.cn)~~

39

40 **Abstract:** Topography and vegetation are critical factors influencing catchment  
41 hydrology; however, their individual contributions are often underestimated in  
42 hydrological models. This limitation is particularly evident in cold, mountainous  
43 regions such as the Mongolian Plateau, where observational data are sparse. To address  
44 this, we employed a stepwise, top-down modelling strategy based on ~~the FLEXa~~  
45 flexible modelling framework to systematically assess the influence of topography and  
46 vegetation on hydrological processes in the Bogd Uliastai and Zavkhan Guulin river  
47 basins. Beginning with a lumped model (FLEX<sup>L</sup>), we successively integrated snow

48 processes (FLEX<sup>L</sup>-S), topographic distribution (FLEX<sup>D</sup>), and finally, a landscape-based  
49 parameterization accounting for vegetation heterogeneity (FLEX<sup>T</sup>). Both FLEX<sup>D</sup> and  
50 FLEX<sup>T</sup> outperformed the lumped models in simulating runoff and ~~SWE~~snow water  
51 equivalent (SWE). Interestingly, FLEX<sup>T</sup> showed similar performance to FLEX<sup>D</sup>—  
52 likely due to limited vegetation heterogeneity—it offers more physically realistic  
53 parameterization by explicitly representing landscape units, suggesting its potential in  
54 more complex basins. ~~Snowmelt contributions~~The ratio of snowmelt runoff to  
55 streamflow ~~were~~was quantified as ~~23.56%±0.7% and 15.9%±1.3% and 14.7%±1.6%~~ in  
56 the Bogd Uliastai and Zavkhan Guulin river basins, respectively, with peaks in spring  
57 and a clear increase with elevation. At high elevations, ~~delayed runoff is primarily~~  
58 ~~snowmelt—resulted-driven, resulting~~ in ~~sustained~~delayed and gradual runoff,  
59 ~~while~~whereas lower elevations ~~responded more rapidly to~~ dominated by rainfall. ~~The~~  
60 ~~explicit representation of vegetation heterogeneity further improved the model's~~  
61 ~~capacity to capture landscape complexity and~~ generate rapid runoff. Controlled by  
62 distinct dominant hydrological mechanisms, different landscape units contribute  
63 unequally to streamflow. This study underscores the pivotal roles of topography and  
64 vegetation in runoff generation and demonstrates the effectiveness of a stepwise  
65 modelling framework for improving hydrological understanding in cryospheric and  
66 data-scarce regions.

67 **Keywords:** Mongolian Plateau, FLEX model, stepwise modelling framework,  
68 snowmelt, topography, vegetation

69

## 70 **1. Introduction**

71 Understanding and accurately simulating hydrological processes are fundamental for  
72 elucidating basin hydrological patterns and supporting water resource management and  
73 ecological protection, ~~especially~~ under ~~the context of~~ global environmental change  
74 ~~(Gomes et al., 2023; Oki and Kanae, 2006)~~(Gomes et al., 2023; Oki and Kanae, 2006).  
75 Topography and vegetation play essential roles as drivers of hydrological processes,  
76 influencing ~~key aspects such as~~ precipitation, interception ~~(Dwarakish and Ganasri,~~

77 ~~2015)(Dwarakish and Ganasri, 2015), snowmelt (Hammond et al., 2019)(Hammond et~~  
78 ~~al., 2019), evaporation (Jiao et al., 2017)(Jiao et al., 2017), and runoff generation (Qin~~  
79 ~~et al., 2025)(Qin et al., 2025). Topography governs water flow paths and moisture~~  
80 ~~release processes (Gao et al., 2014), while vegetation affects water movement and~~  
81 ~~infiltration by regulating precipitation interception and soil moisture dynamics (Zhu et~~  
82 ~~al., 2022). The complex interaction between topography and vegetation not only define~~  
83 ~~Hydrological Response Units (HRUs) but also shape the spatial heterogeneity and~~  
84 ~~dominant hydrological mechanisms within a river basin (Savenije, 2010; Sivapalan,~~  
85 ~~2009). However, in cold arid regions, data scarcity often leads to oversimplified~~  
86 ~~hydrological models, limiting accurate simulations (Ragetti et al., 2014; Tarasova et~~  
87 ~~al., 2016). Therefore, a more comprehensive evaluation of topography-vegetation~~  
88 ~~interactions is essential for improving model fidelity and supporting effective water~~  
89 ~~resource management and ecological conservation. Their combined influence~~  
90 ~~underpins landscape organization, forms the basis for Hydrological Response Units~~  
91 ~~(HRUs), and shapes spatial heterogeneity and dominant hydrological mechanisms~~  
92 ~~(Savenije, 2010; Sivapalan, 2009). Limited observational data in cold-arid regions often~~  
93 ~~results in oversimplified hydrological models, emphasizing the need to represent~~  
94 ~~landscape controls more explicitly (Ragetti et al., 2014; Tarasova et al., 2016).~~

95  
96 ~~Topography plays a fundamental role in governs water redistribution across landscapes~~  
97 ~~by shaping hydrological processes by influencing the spatial distribution of soil~~  
98 ~~moisture, regulating precipitation patterns, modulating precipitation and evaporation~~  
99 ~~dynamics, and drivingcontrolling runoff generation, thereby governing the movement~~  
100 ~~and storage of water across the landscape pathways (Wicki et al., 2023)(Wicki et al.,~~  
101 ~~2023). In mountainous basins, variations in topographiestrong relief~~  
102 ~~introduceeintroduces substantial uncertainty intochallenges for hydrological modeling~~  
103 ~~modelling and increase predictive uncertainty (Seibert and McDonnell, 2002)(Seibert~~  
104 ~~and McDonnell, 2002). Steeper slopes typically lead to more rapid runoff, while gentler~~  
105 ~~slopes promote greater infiltration and moisture retention, thusthereby affecting the~~

106 ~~spatial and temporal~~spatiotemporal distribution of water resources (~~Ye et al., 2023~~)(Ye  
107 et al., 2023). Moreover, ~~topography critically influences snow distribution and~~  
108 ~~snowmelt dynamics. Terrain~~In addition, topographic features such as slope, aspect, and  
109 elevation ~~induce spatial heterogeneity in~~control snow accumulation and ~~melting~~  
110 ~~processes~~melt, resulting in ~~diverse~~highly heterogeneous hydrological responses across  
111 ~~the basin~~basins (~~Broxton et al., 2020~~)(Broxton et al., 2020).

112  
113 Vegetation ~~plays a crucial role in regulating~~also regulates hydrological processes;  
114 ~~particularly through interception by~~intercepting snow and ~~root zone water storage. First,~~  
115 ~~vegetation canopies intercept rainfall, reducing the amount of~~facilitating water  
116 infiltration and storage in the root zone, and absorbing and transpiring water through  
117 its roots. Canopies reduce effective precipitation reaching the soil, ~~while also~~  
118 ~~mitigating~~ground and can mitigate surface ~~erosion and slowing~~ runoff (~~Cheng et al.,~~  
119 ~~2020~~)(Cheng et al., 2020). ~~Second, while~~ root ~~zone storage capacity and plant~~  
120 ~~transpiration regulates~~systems shape soil moisture, ~~enhance evaporation dynamics and~~  
121 ~~facilitating~~ water redistribution (~~Luo et al., 2022; Volpe et al., 2013~~)(Luo et al., 2022;  
122 Volpe et al., 2013). ~~These effects vary by~~ Consequently, different vegetation ~~type, as~~  
123 ~~different structural form~~types (e.g., forests ~~vs. grasslands~~), grassland, and abandoned  
124 farmland ~~often~~ exhibit distinct hydrological behaviors (~~Chen et al., 2023~~)(Chen et al.,  
125 2023). In cold mountainous regions, vegetation ~~also affects~~further alters snow  
126 processes ~~by affecting snow distribution~~through shading and retention. For example,  
127 ~~forest canopies can shield snow accumulation, delay snowmelt, and reduce~~moderating  
128 ~~wind-driven~~ redistribution, thereby ~~significantly altering~~influencing the ~~spatiotemporal~~  
129 ~~dynamics of meltwater runoff~~timing and magnitude (~~Sun et al., 2022~~)(Sun et al., 2022).  
130 Over long timescales, snow-vegetation interactions can modulate runoff sensitivity to  
131 precipitation, evapotranspiration, and vegetation dynamics, especially in regions such  
132 as Central Asia (Feng et al., 2025) and the Tibetan Plateau (Ni et al., 2025).

133  
134 Despite -

135

136 Although the regulatory role of topography and vegetation in basin hydrology are  
137 widely acknowledged,, their synergistic interactions remain insufficiently understood,  
138 particularly in cold high-altitude mountainous regions characterized by complex terrain,  
139 harsh climatic conditions, and limited observational data (Stephens et al., 2021).  
140 Cryospheric regions serve as critical freshwater resources for downstream areas and are  
141 especially sensitive to changes in the hydrological cycle and climate (Immerzeel et al.,  
142 2010). In these regions, snowfall and snowmelt processes often dominate runoff  
143 generation, with topography and vegetation jointly modulating hydrological responses  
144 by influencing snow distribution, accumulation, and melt rates (Dharmadasa et al.,  
145 2023; Zhong et al., 2021). Therefore, quantifying the individual and combined effects  
146 of topography and vegetation, and effectively integrating them into hydrological  
147 models, is essential for advancing cold-region hydrology.

148  
149 Existing hydrological models often struggle to adequately capture the complexities  
150 introduced by topography and vegetation. Early lumped models typically used basin-  
151 averaged precipitation and temperature to simulate runoff, thereby oversimplifying  
152 spatial heterogeneity within catchments (Beven, 2012). While computationally efficient,  
153 lumped models fail to accurately represent the spatial variability of terrain and land  
154 cover, especially in mountainous regions. The advent of distributed hydrological  
155 models has allowed more spatially explicit simulations by incorporating topographic  
156 and land cover data (Fenicia et al., 2016). However, the performance of these models  
157 is highly dependent on data quality, which remains a significant limitation in cold, high-  
158 mountain regions where traditional observations are sparse or unavailable.

159  
160 Remote sensing has become an invaluable tool for providing high-resolution data on  
161 topography, vegetation, and snow in hydrological studies of cold regions. Digital  
162 elevation models (DEMs) offer critical topographic information such as slope, aspect,  
163 and elevation, while vegetation indices derived from remote sensing (e.g., NDVI and  
164 EVI) effectively characterize vegetation cover (Xiong et al., 2023). In addition, remote  
165 sensing techniques enable spatial monitoring of snow water equivalent and snowmelt

166 processes (Duethmann et al., 2014). Integrating remote sensing data with distributed  
167 hydrological models helps to overcome the limitations of traditional in situ  
168 observations, offering a more comprehensive understanding of the roles that  
169 topography and vegetation play in shaping hydrological processes (Gao et al., 2014).

170  
171 In the absence of direct measurements of individual hydrological processes, the top-  
172 down modelling approach offers a powerful means of exploring the internal dynamics  
173 of basin behavior (Fenicia et al., 2008b). Originally proposed by Klemes (Klemeš, 1983)  
174 and later reformulated by Sivapalan et al. (Sivapalan et al., 2003), the top-down  
175 approach is rooted in a deductive philosophy that infers the underlying ‘causes’ from  
176 the overall observed ‘effect’ of a system. In hydrological modeling, this method begins  
177 with a simple structure that is progressively refined to address limitations in  
178 reproducing observed catchment behavior (Fenicia et al., 2008a). In cold mountainous  
179 regions, the top-down approach holds significant potential for improving model realism  
180 by systematically incorporating key variables such as snow processes, topography, and  
181 vegetation.

182  
183 This study focuses on the Bogd Uliastai and Zavkhan Guulin river basins on the  
184 Mongolian Plateau, aiming to investigate the roles of topography and vegetation in  
185 shaping hydrological processes in cold mountainous regions. Due to the scarcity of  
186 observational data, traditional hydrological models face significant challenges in these  
187 areas. To address this, we employ a top-down modelling approach, beginning with a  
188 lumped model to assess runoff dynamics and progressively advancing toward a  
189 distributed framework. This model explicitly incorporates key components—including  
190 snowmelt, topography, and vegetation—to better capture the hydrological responses of  
191 different landscape units. The study seeks to address three key research questions: (1)  
192 the recognized importance of topography and vegetation, their influences remain  
193 insufficiently represented in many hydrological modelling frameworks (Stephens et al.,  
194 2021). This gap is especially critical in cryospheric regions, where snow accumulation

195 and melt dominate runoff generation and are strongly shaped by terrain and vegetation  
196 controls (Dharmadasa et al., 2023; Immerzeel et al., 2010; Zhong et al., 2021).  
197 Quantifying and integrating these controls into hydrological models is therefore  
198 essential for advancing cold-region hydrology and improving model realism.

199  
200 Existing hydrological models often struggle to adequately capture the complexities  
201 introduced by topography and vegetation heterogeneity. Early lumped models, relying  
202 on basin-averaged inputs, oversimplify spatial heterogeneity within catchments (Beven,  
203 2012). Distributed hydrological models allow spatially explicit simulations but are  
204 highly dependent on the availability and quality of input data (Fenicia et al., 2016),  
205 which remains a significant limitation in cold, high-mountain regions. Remote sensing  
206 has become an invaluable tool for providing spatially continuous data on topography  
207 (e.g., Digital Elevation Models, DEMs), vegetation (e.g., Normalized Difference  
208 Vegetation Index (NDVI) and Enhanced Vegetation Index (EVI)) (Xiong et al., 2023),  
209 and snow dynamics (e.g., SWE) (Duethmann et al., 2014), enabling a more realistic  
210 representation of landscape-dependent controls in hydrological models (Gao et al.,  
211 2014).

212  
213 In the absence of direct measurements of individual hydrological processes, the top-  
214 down modelling approach offers a powerful and practical means of exploring the  
215 internal dynamics of basin behavior (Fenicia et al., 2008b). Originally proposed by  
216 Klemeš (Klemeš, 1983) and later reformulated by Sivapalan et al. (Sivapalan et al.,  
217 2003), the top-down approach is rooted in a deductive philosophy that infers the  
218 underlying ‘causes’ from the overall observed ‘effect’ of a system. In hydrological  
219 modelling, this method begins with a simple structure that is progressively refined to  
220 address limitations in reproducing observed catchment behavior (Fenicia et al., 2008a).

221  
222 The Bogd Uliastai and Zavkhan Guulin river basins, in the headwaters of the Zavkhan  
223 River on the western Mongolian Plateau, exhibit a cold, arid continental climate with

224 sparse vegetation (Baasanmunkh et al., 2019). Strong cryospheric influences control  
225 hydrological processes, making these basins key areas for regional ecological security  
226 and downstream water-resource resilience. However, monitoring networks are sparse  
227 and long-term observational data are limited, leaving runoff generation mechanisms  
228 and their interactions with topography, vegetation and the cryosphere poorly understood  
229 (Dorjsuren et al., 2024).

230  
231 To address these challenges, we employ a top-down modelling framework that begins  
232 with a lumped model to assess runoff dynamics and progressively incorporates  
233 distributed representations of snowmelt, topography, and vegetation. This framework  
234 allows assessment of hydrological responses across different landscape units and  
235 addresses three research questions:

236 (1) How can runoff be effectively simulated in data-scarce, cold mountainous regions  
237 using a top-down modelling approach? (2)–

238 (2) How can the contribution of snowmelt runoff to streamflow be quantified  
239 through using a landscape-based hydrological model? (3)–

240 (3) How do topography and vegetation influence runoff generation processes?

241  
242 The study aligns with the IAHS HELPING Decade (Hydrology Engaging Local People  
243 IN one Global world, 2023–2032), which calls for interdisciplinary research in data-  
244 scarce and ecologically vulnerable regions. By developing a modelling framework for  
245 cold basins with limited observational data and improving understanding of  
246 hydrological processes on the Mongolian Plateau, this work provides an important case  
247 study contributing to the goals of the HELPING initiative.

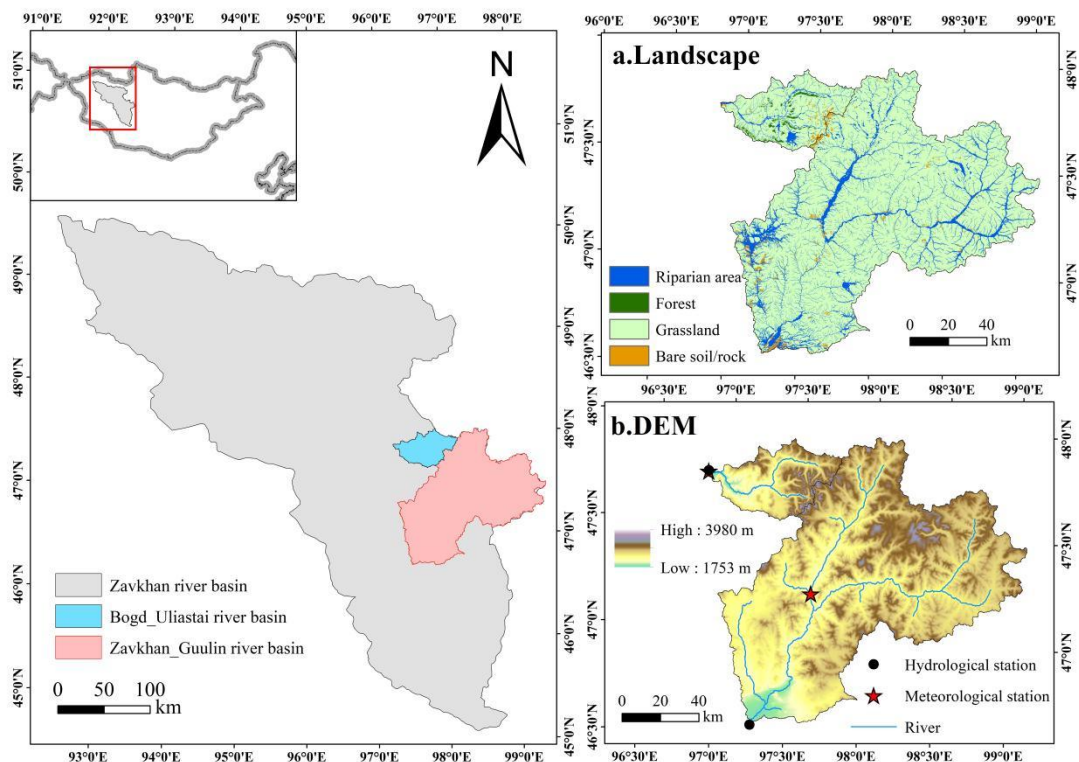
## 249 **2. Study site**

### 250 **2.1 Bogd Uliastai river basin**

251 The Bogd Uliastai river basin (47°30'N-48°10'N, 96°45'E-97°45'E) is located in the

252 northern part of the Zavkhan river headwaters, along the southern foothills of the central  
 253 Khangai Mountains in Mongolia (Fig.1). The basin spans an area of 1610 km<sup>2</sup> and is  
 254 predominantly mountainous, with elevations ranging from 1753 m a.s.l. to 3972 m a.s.l.  
 255 The region receives an average annual precipitation of approximately 200 mm, with  
 256 more than 80% of rainfall occurring between June and September. The average annual  
 257 temperature is -1°C, while winter temperatures frequently fall below -30°C, reflecting  
 258 a typical alpine climate. Runoff displays strong seasonal variability, with distinct peaks  
 259 during the spring and summer and almost no flow in winter, resulting in extreme  
 260 hydrological conditions (Dorjsuren et al., 2024)(Dorjsuren et al., 2024). The vegetation  
 261 exhibits clear altitudinal zonation: alpine meadows and tundra, dominated by mosses  
 262 and lichens, prevail at higher elevations, whereas needlegrass steppe and low  
 263 shrublands are common in mid- and low- elevation zones/areas (Baasanmunkh et al.,  
 264 2019)(Baasanmunkh et al., 2019).

265



266

267 **Fig.1** Location, landscape (a) and topography (b) of the Bogd Uliastai and Zavkhan Guulin river  
 268 basins on the Mongolian Plateau.

269

## 270 **2.2 Zavkhan Guulin river basin**

271 The Zavkhan Guulin river basin (46°30'N-47°50'N, 96°45'E-97°00'E), located in the  
272 central and southern parts of Zavkhan Province, lies within the transitional zone of the  
273 southern Khangai Mountains (Fig.1). The basin covers an area of approximately 12258  
274 km<sup>2</sup> and is predominantly composed of low mountains and hills, with elevations  
275 ranging from 1785 m a.s.l. to 3980 m a.s.l. The basin's annual average precipitation is  
276 about 160 mm, with most precipitation concentrated in ~~the summer, primaril in the form~~  
277 ~~of heavy rain, which serves the main source of runoff.~~summer. The annual average  
278 temperature is approximately -3°C, with summer temperatures exceeding 20°C and  
279 winter temperatures dropping as low as -50°C, characteristic of a temperate continental  
280 climate (~~Dorjsuren et al., 2023~~)(Dorjsuren et al., 2023). Vegetation in the region is  
281 sparse, primarily dominated by drought-tolerant *Artemisia* species, with scattered  
282 distributions of grass and shrubs. At higher elevations, the landscape is characterized  
283 by alpine meadows, exposed rock surfaces, and cold desert environments. Soils are  
284 nutrient-poor, and the ecological environment is fragile, facing severe challenges such  
285 as soil erosion (~~Baasanmunkh et al., 2019~~)(Baasanmunkh et al., 2019).

286

## 287 **3. Data**

### 288 **3.1 Data set**

289 **Hydrometeorological data:** Daily precipitation, runoff, and temperature data for the  
290 Bogd Uliastai river basin (2007–2015) and the Zavkhan Guulin river basin (2000–2020)  
291 were obtained from the Information and Research Institute of Meteorology, Hydrology,  
292 and Environment (IRIMHE) via its official website (<http://irimhe.namem.gov.mn>). For  
293 each basin, one meteorological station and one hydrological station served as the  
294 primary sources of observational data. The Arctic Snow Water Equivalent (SWE) Grid  
295 Dataset (2003–2016) was obtained from National Tibetan Plateau/Third Pole  
296 Environment Data Center (<https://cstr.cn/18406.11.Snow.tpd.c.271556>). The SWE  
297 product has a daily temporal resolution and a spatial resolution of 10 km, covering

298 latitudes from 45°N to 90°N and longitudes from 180°W to 180°E.

299 **Topographic data:** The Shuttle Radar Topography Mission Digital Elevation Model  
300 (SRTM-DEM), with a spatial resolution of 90 m, was acquired from the official website  
301 of the ~~International Center for Tropical Agriculture~~[CGIAR Consortium for Spatial  
302 Information \(CGIAR-CSI\)](http://srtm.csi.cgiar.org) (<http://srtm.csi.cgiar.org>).

303 **Land cover data:** The Sentinel-2 10-Meter Land Use/Land Cover was accessed via  
304 ESRI's official platform (<https://livingatlas.arcgis.com/landcover/>).

305 **NDVI data:** The normalized difference vegetation index (NDVI) data (2013–2020)  
306 were derived from the Landsat 8 Operational Land Imager (OLI) Level-2 surface  
307 reflectance products. NDVI was calculated as  $(\text{NIR} - \text{Red})/(\text{NIR} + \text{Red})$  using bands  
308 5 (NIR) and 4 (Red). The dataset has a spatial resolution of 30 m and a temporal  
309 resolution of 16 days. Landsat data were obtained from the United States Geological  
310 Survey (USGS) EarthExplorer platform (<https://earthexplorer.usgs.gov/>).

311

### 312 **3.2 Distribution of forcing data**

313 Mountainous terrain is complex, and meteorological stations are typically located at  
314 lower elevations. Directly using point-based measurement in basin-scale simulations  
315 without accounting for elevation effects can introduce biases (~~Klemeš, 1989~~)([Klemeš,  
316 1989](#)). In cold mountainous regions, higher elevations typically experience lower  
317 temperatures and greater precipitation, often in the form of snow (~~Lundquist et al., 2010;  
318 Stahl et al., 2006~~)([Lundquist et al., 2010; Stahl et al., 2006](#)). In the study, the ~~FLEX  
319 model divides~~[FLEX<sup>D</sup> and FLEX<sup>T</sup> models divide](#) catchment into elevation bands and  
320 adjusts temperature and precipitation for each band using a precipitation increase rate  
321 and temperature lapse rate: ([Fig.2](#)). This distributed input approach effectively mitigates  
322 simulation bias by better capturing altitudinal variability in meteorological conditions.  
323 In this study, due to the remoteness of the region and the sparse distribution of  
324 meteorological stations, available ground observations were limited. Satellite and  
325 reanalysis products (e.g., ERA5-[Land](#)) exhibit notable biases over complex terrain and

fail to capture local climatic variability. We therefore ~~relied on the best available in-situ data, which were subjected to rigorous quality control and spatial interpolation, and supplemented by topographic context and previous studies. While uncertainties remain, this approach provides the most reliable climate forcing achievable under current observational constraints.~~ used the nearby Tsagan-Turutuin-gol catchment as a reference, which also originates in the Khangai Mountains and shares similar topographic and climatic characteristics with the study basins (Klimek and Starkel, 1980). The model employed a precipitation increase rate of 4.2% per 100 m and a temperature lapse rate of 0.6°C per 100 m (Gao et al., 2014).

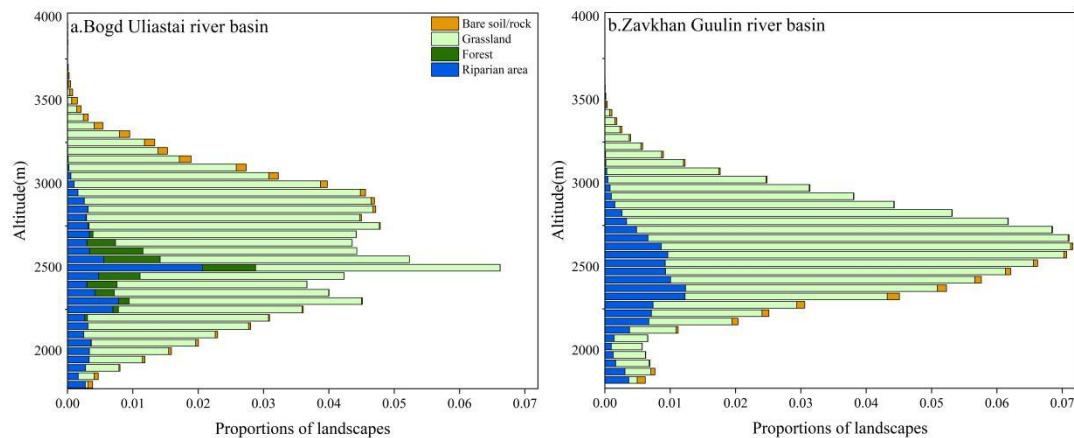
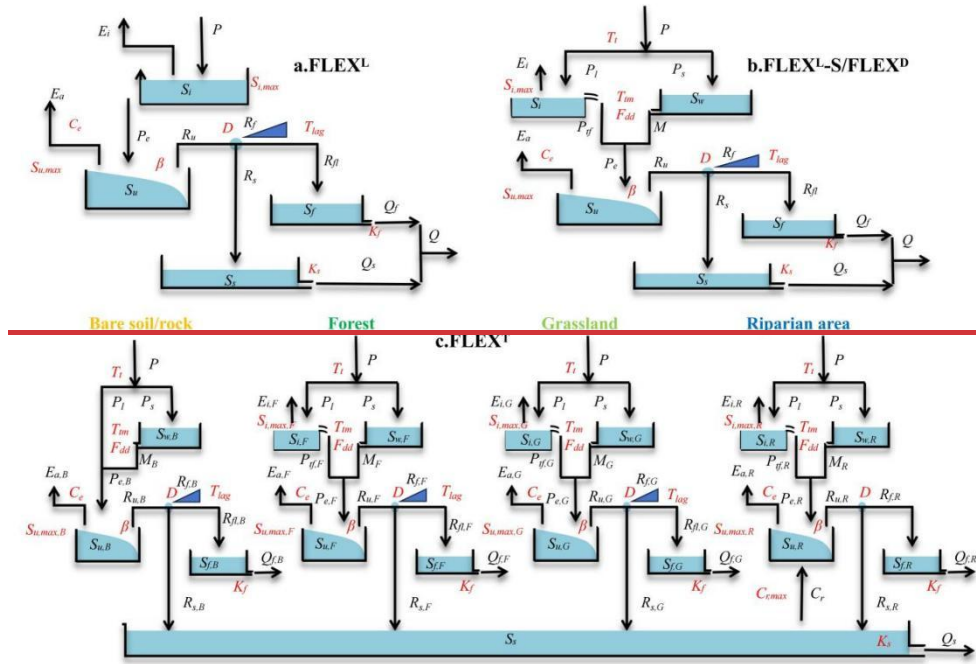


**Fig.2** Area of different elevation and landscape in Bogd Uliastai and Zavkhan Guulin river basins.

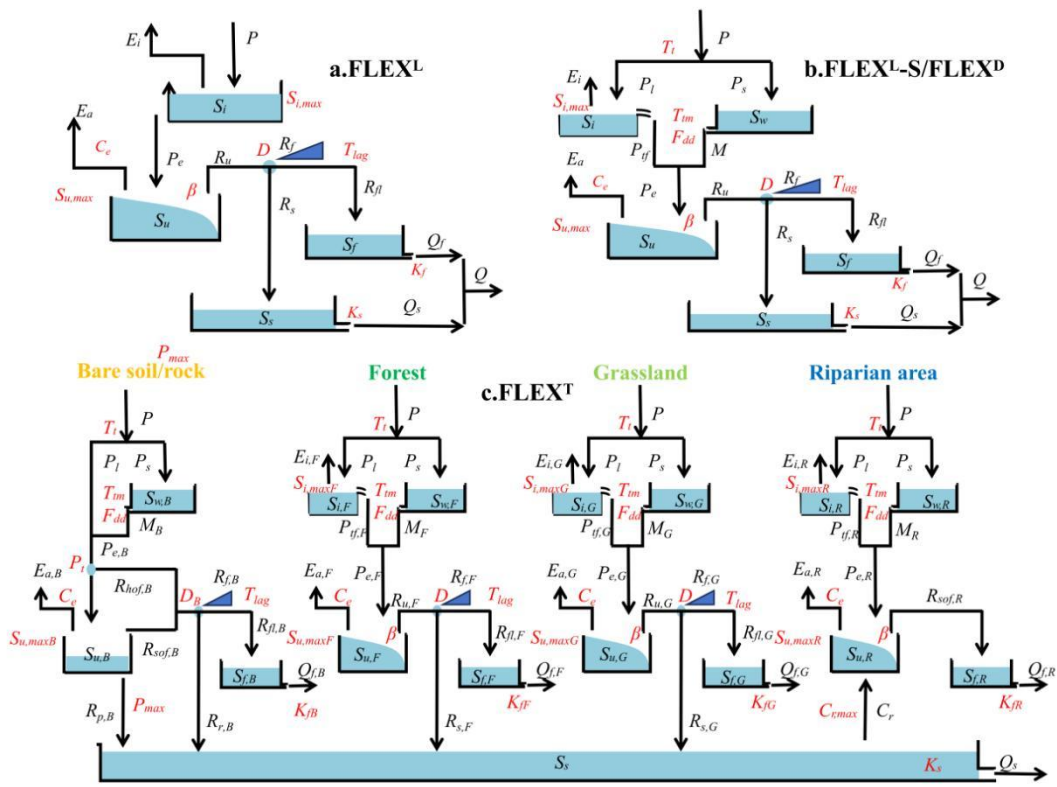
## 4. Modelling approach

### 4.1 Model description

To assess the impact of topography and vegetation on hydrological processes, this study designed and tested four conceptual models with increasing complexity: FLEX<sup>L</sup>, FLEX<sup>L-S</sup>, FLEX<sup>D</sup>, and FLEX<sup>T</sup> (Fig.2). The model structure and variables are shown in Fig. 23 and Table 1, and the water balance, isotope mass balance and constitutive equations are shown in Table 2.



346



347

348 **Fig.23** Stepwise modelling and the model structure of four models. (a) FLEX<sup>L</sup> is a lumped model  
 349 without snow module; (b) FLEX<sup>L-S</sup> is a lumped model with snow module, and FLEX<sup>D</sup> is a semi-  
 350 distributed model with the same structure as FLEX<sup>L-S</sup>. (c) FLEX<sup>T</sup> is a landscape-driven semi-  
 351 distributed model.

352

353 **Table1.** The variables of four models. In FLEX<sup>T</sup> model, variables associated with various landscape  
 354 categories are differentiated using specific suffixes, e.g.,  $E_{i,F}$ , represent the interception from forest.

Variables	Meaning	Variables	Meaning
$P$ (mm/d)	Precipitation	$E_i$ (mm/d)	Interception
$S_i$ (mm)	Interception reservoir	$P_s$ (mm/d)	Snowfall
$P_l$ (mm/d)	Rainfall	$P_{tf}$ (mm/d)	Effective rainfall after interception
$M$ (mm/d)	Snowmelt	$P_e$ (mm/d)	Effective precipitation
$S_u$ (mm)	<del>Unsaturated</del> Root zone reservoir	$E_a$ (mm/d)	Actual evaporation
$R_u$ (mm/d)	Generated runoff from the <del>unsaturated</del> root zone reservoir	$R_f$ (mm/d)	Generated fast runoff <del>in the</del> <del>unsaturated zone</del>
$R_{fl}$ (mm/d)	Discharge into the fast response reservoir after the convolution	$R_s$ (mm/d)	Generated slow runoff <del>in the</del> <del>unsaturated zone</del>
$R_{hor}$ (mm/d)	<u>Hortonian overland flow from bare soil/rock</u>	$R_p$ (mm/d)	<u>Deep percolation from bare soil/rock</u>
$R_{sor}$ (mm/d)	<u>Saturation overland flow</u>	$R_r$ (mm/d)	<u>Water re-infiltrating</u>
$S_f$ (mm)	Fast response reservoir	$S_s$ (mm)	Slow response reservoir
$C_r$ (mm/d)	Capillary rise from groundwater into <del>unsaturated</del> root zone reservoir on riparian area	$Q_f$ (mm/d)	<del>Subsurface</del> <u>Surface flow</u> /subsurface storm flow
$Q_s$ (mm/d)	Groundwater flow	$Q$ (mm/d)	Total runoff

355

356

357

358 **Table 2.** The water balance and constitutive equations used in four models. Note: FLEX<sup>L</sup> model lacks the snow module, resulting in different water balance and  
359 structural equations compared to other models. For FLEX<sup>T</sup> model, in Eqs (4), (6), 7 and (7), 9, the  $S_i$  and  $S_{i,max}$  represent the interception reservoir and its interception  
360 capacities, respectively, for different landscapes/units, including forest ( $S_{i,max,F}$ ), grassland ( $S_{i,max,G}$ ) and riparian area ( $S_{i,max,R}$ ). (There is  
361 no  $S_{i,max}$ ). No interception reservoir is defined for bare soil/rock areas. Similarly, in Eqs. (8), (10), (11), and (12), the  $S_u$  and  $S_{u,max}$  represent  
362 zone reservoirs and their corresponding storage capacities for different landscapes, including bare soil/rock ( $S_{u,max,F}$ ), forest ( $S_{u,max,F}$ ), grassland ( $S_{u,max,G}$ ) and riparian  
363 area ( $S_{u,max,R}$ ), while  $K_r$  represents the recession coefficient of the fast response reservoir for each landscape type.

Reservoirs	Water balance equations	Constitutive equations
Interception reservoir (FLEX <sup>L</sup> )	$\frac{dS_i}{dt} = P - E_i - P_e$ (1)	$E_i = \min(E_p, \min(P, S_{i,max}))$ (2) $P_e = \max(P - E_i, 0)$ (3)
Snow reservoir (FLEX <sup>L</sup> -S/FLEX <sup>D</sup> /FLEX <sup>T</sup> )	$\frac{dS_w}{dt} = P_s - M$ (4)	$P_s = \begin{cases} P; & T < T_t \\ 0; & T \geq T_t \end{cases}$ (5) $M = \begin{cases} F_{dd}(T - T_{tm}); & T > T_{tm} \\ 0; & T \leq T_{tm} \end{cases}$ (6)
Interception reservoir (FLEX <sup>L</sup> -S/FLEX <sup>D</sup> /FLEX <sup>T</sup> )	$\frac{dS_i}{dt} = P_l - E_i - P_{tf}$ (7)	$P_l = \begin{cases} P; & T \geq T_t \\ 0; & T < T_t \end{cases}$ (8) $E_i = \min(E_p, \min(P_l, S_{i,max}))$ (9) $P_{tf} = \max(P_l - E_i, 0)$ (10)

---


$$P_e = P_{tf} + M \quad (11)$$

$$\frac{dS_u}{dt} = P_e - E_a - R_u \quad (12)$$

$$E_a = (E_p - E_i) \min\left(\frac{S_u}{c_e S_{u,max}}, 1\right) \quad (13)$$

$$R_u = \begin{cases} P_e - S_{u,max} + S_u + S_{u,max} \left(1 - \frac{P_e + AU}{(1+\beta)S_{u,max}}\right)^{(1+\beta)} & ; (1+\beta)S_{u,max} > P_e + AU \\ P_e - S_{u,max} + S_u & (1+\beta)S_{u,max} \leq P_e + AU \end{cases} \quad (14)$$

(All)

$$AU = (1+\beta)S_{u,max} \left(1 - \left(1 - \frac{S_u}{S_{u,max}}\right)^{\frac{1}{1+\beta}}\right) \quad (15)$$

$$R_f = R_u D \quad (16)$$

$$R_s = R_u(1 - D) \quad (17)$$

$$R_{rl} = \sum_{i=1}^{T_{lag}} c(i) \cdot R_f(t - i + 1) \quad (18)$$

$$c(i) = i / \sum_{u=1}^{T_{lag}} u \quad (19)$$

$$Q_f = S_f / K_f \quad (21)$$

$$\frac{dS_f}{dt} = R_f - Q_f \quad (20)$$

$$Q_s = S_s / K_s \quad (23)$$

$$\frac{dS_s}{dt} = R_s - Q_s \quad (22)$$

Splitter and lag function (All)

Fast reservoir (All)

Slow reservoir (All)

### 365 4.1.1 FLEX<sup>L</sup>

366 FLEX<sup>L</sup> is a lumped conceptual hydrological model composed of four reservoirs  
367 (Fig.2a3a): an interception reservoir ( $S_i$ ), ~~an~~ unsaturated root zone reservoir ( $S_u$ ), a fast  
368 response reservoir ( $S_f$ ), and a slow response reservoir ( $S_s$ ). A lag function is used to  
369 represent the lag time from storm to peak flow ( $T_{lag}$ ). FLEX<sup>L</sup> includes a total of 8 free  
370 calibration parameters (Table 3).

371

372 The interception reservoir was designed to simulate the process of precipitation  
373 interception by vegetation canopies or the ground surface (Eq.1). Interception  
374 evaporation ( $E_i$ ) was calculated by potential evaporation ( $E_p$ ) and  $S_i$ , considering the  
375 interception storage capacity ( $S_{i,max}$ ) (Eq.2). When precipitation ( $P$ ) exceeds  $S_{i,max}$ , the  
376 excess precipitation is routed as effective precipitation ( $P_e$ ) into the unsaturated root  
377 zone reservoir (Eq.3).

378

379 In the unsaturated root zone reservoir, actual evaporation ( $E_a$ ) was estimated based on  
380  $E_p - E_i$  and root zone soil moisture ( $S_u/S_{u,max}$ ) (Eq.13). The parameter  $C_e$  represents the  
381 threshold value controlling evaporation from the root zone soil moisture, and  $S_{u,max}$  is  
382 root zone storage capacity. The water retention curve from the Xin'anjiang model was  
383 used to partition  $P_e$  into stored water in  $S_u$  and runoff generated from the unsaturated  
384 root zone ( $R_u$ ) (Eqs.14 and 15) (Zhao, 1992)(Zhao, 1992)-(Eqs.14 and 15)-.

385

386 In the response reservoir, a splitter  $D$  was applied to divide the  $R_u$  into two fluxes ( $R_f$   
387 and  $R_s$ ) (Eqs.16 and 17), and Eqs (18) and (19) were used to describe the lag time  
388 between storm and peak flow.  $R_f(t-i+1)$  represents the fast runoff generated in the  
389 unsaturated root zone at time  $t-i+1$ ,  $T_{lag}$  represents the time lag between the storm and  
390 fast runoff generation.  $c(i)$  is the weight of the flow in  $i-1$  days before and  $R_f(t)$  is the  
391 discharge into the fast response reservoir after convolution. We used two linear  
392 reservoirs to represent the response process of subsurface storm flow ( $Q_f$ ) and  
393 groundwater flow ( $Q_s$ ) (Eqs.21 and 23).

394

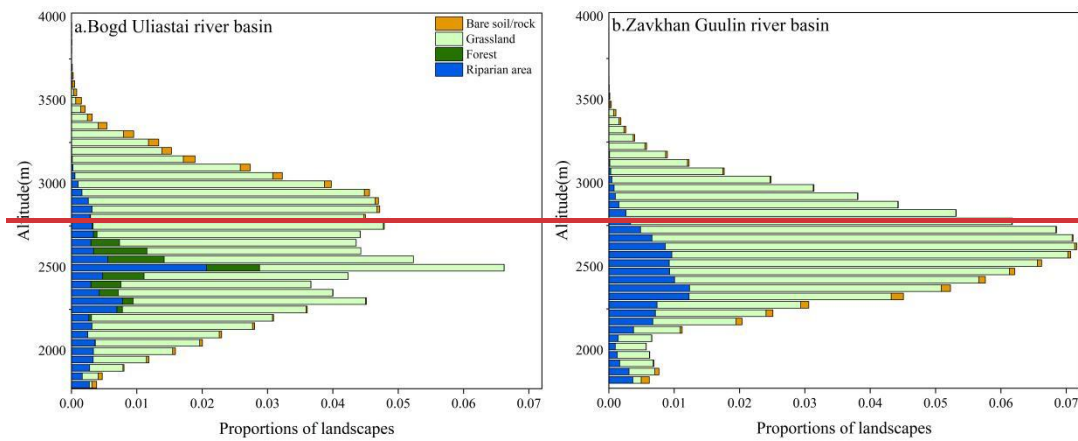
### 395 **4.1.2 FLEX<sup>L</sup>-S**

396 FLEX<sup>L</sup>-S builds upon the FLEX<sup>L</sup> model by incorporating a snow reservoir ( $S_w$ ) to  
397 simulate the snow accumulation and melt processes (Fig.2b3b). When the daily air  
398 temperature exceeds the threshold temperature ( $T_t$ ) and there is no snowpack (typically  
399 in summer), the interception process governs the initial partitioning of precipitation  
400 (Eq.7). In contrast, when the daily mean temperature is below  $T_t$  (normally occurs in  
401 winter), precipitation is stored as snow (Eq.5). When there is snowpack and the daily  
402 air temperature is above  $T_t$  (normally prevailing in early spring and early autumn),  
403 effective precipitation ( $P_e$ ) is equal to the sum of effective rainfall after interception ( $P_{if}$ )  
404 and snowmelt ( $M$ ) (Eq.11).  $M$  was calculated by the snow degree day factor ( $F_{dd}$ ) and  
405 the threshold temperature for melting ( $T_{tm}$ ) (Eq.6) (Gao et al., 2017)(Gao et al., 2017).  
406 In this study,  $T_{tm}$  was set to the same value as  $T_t$ . It is important to note that meltwater  
407 is conceptualized as directly infiltrating into the soil, thereby bypassing the interception  
408 reservoir.

409

### 410 **4.1.3 FLEX<sup>D</sup>**

411 FLEX<sup>D</sup> is a semi-distributed model with the same structure and parameters as FLEX<sup>L</sup>-  
412 S (Fig.2b3b). Using DEM data, the Bogd Uliastai river basin was divided into 45  
413 elevation bands with 50 m interval, while the Zavkhan Guulin river basin was divided  
414 into 44 elevation bands as shown in Fig.32. The FLEX<sup>D</sup> model was operated with semi-  
415 distributed input data (see Sect.3.2), ensuring the integration of spatial variability into  
416 the model's processes.



417  
418 **Fig.3** Area of different elevation and landscape in Bogd Uliastai and Zavkhan Guulin river basins.

#### 419 **4.1.4 FLEX<sup>T</sup>**

420 The FLEX<sup>T</sup> model classified the Bogd Uliastai river basin into four landscape  
421 elements—bare soil/rock, forest, grassland, and riparian area—based on vegetation  
422 characteristics. In contrast, the Zavkhan Guulin river basin, which has no forest, was  
423 categorized into three landscape elements. By integrating both landscape types and  
424 elevation bands, the Bogd Uliastai river basin was further subdivided into 132 HRUs,  
425 while the Zavkhan Guulin river basin consisted of 117 HRUs (Fig.32).

426  
427 The FLEX<sup>T</sup> model's structure comprised four parallel components, representing the  
428 distinct hydrological functions associated with landscape elements (Savenije, 2010;  
429 Gao et al., 2014) (Fig.2e). (Gao et al., 2014). To capture the diverse rainfall-runoff  
430 processes in different landscape types ~~and simultaneously avoid over-parameterization,~~  
431 ~~we kept the same model structure but gave different interception storage capacity ( $S_{i,max}$ )~~  
432 ~~and root zone storage capacity ( $S_{u,max}$ ) for all, landscape elements (Table 3).~~

433  
434 ~~For forest, due to their dense vegetation cover and the greater amount of water required~~  
435 ~~to fill the root zone to meet water deficits, larger prior ranges~~ were assigned to  
436  ~~$S_{i,maxF}$  model structures (Fig.3c) and  $S_{u,maxF}$  parameters (Table 3) tailored to their~~  
437 ~~dominant hydrological processes.~~

438  
439 For bare soil/ ~~and~~ rock, ~~due to no areas,~~ vegetation cover, we constrained a shallower

440  ~~$S_{u,maxB}$  and did not incorporate an~~ is absent; therefore, no interception module occurs.  
441 Due to the low infiltration capacity of these surfaces, Hortonian overland flow ( $R_{hof,B}$ )  
442 dominates runoff generation when daily effective precipitation ( $P_{e,B}$ ) exceeds the  
443 threshold parameter ( $P_t$ ) (Eq. 24):

$$444 R_{hof,B} = \max(P_{e,B} - P_t, 0) \quad (24)$$

445 Saturation overland flow ( $R_{sof,B}$ ), , caused by the limited storage capacity of shallow  
446 soils, occurs when the unsaturated zone soil moisture reaches its maximum storage  
447 capacity ( $S_{u,maxB}$ ). Deep percolation into groundwater ( $R_{p,B}$ ) is governed by relative soil  
448 moisture ( $S_{u,B}/S_{u,maxB}$ ) and the maximum percolation ( $P_{max}$ ; Eq. 25). Surface runoff is  
449 further partitioned into re-infiltrating water ( $R_{r,B}$ ) over high-permeability debris slopes  
450 and water routed directly to the channel ( $R_{f,B}$ ) through a separator ( $D_B$ ).

$$451 R_{p,B} = P_{max} \frac{S_u}{S_{u,max}} \quad (25)$$

452  
453 Forest and grassland hillslopes follow the same FLEX<sup>D</sup> model structure, with  
454 differences represented through parameters governing interception and root zone  
455 processes.

456  
457 For the riparian area, which is prone to saturation due to its location, we also constrained  
458 a shallower  $S_{u,maxR}$ , with the effect of capillary rise ( $C_r$ ) taken into account.  $C_r$  is  
459 represented by a parameter ( $C_{r,max}$ ) indicating a constant amount of capillary rise.

460 ~~Notably, the~~ The lag time from storm to peak flow was not considered in riparian area.

461 ~~For~~

462  
463 Interception thresholds were parameterized to be highest for forest ( $S_{i,maxF}$ ), followed  
464 by grassland ( $S_{i,maxG}$ ) and riparian area ( $S_{i,maxR}$ ), reflecting differences in canopy  
465 interception capacity.

466 The root zone storage capacity was assigned deepest in forests ( $S_{u,maxF}$ ), shallower in  
467 grasslands,  ~~$S_{u,maxG}$  is lower~~ ( $S_{u,maxG}$ ), and smallest in riparian areas ( $S_{u,maxR}$ ). Bare soil  
468 and rock ( $S_{u,maxB}$ ) were represented as belonging to the unsaturated zone rather than the

469 root zone, with storage capacity similar to that of forest but higher than riparian areas.  
470 Response timescales were parameterized to be longest for groundwater ( $K_s$ ), shortest  
471 for saturation-excess runoff in riparian area ( $K_R$ ) and surface runoff in bare soil/rock  
472 and riparian area.

473 ( $K_{fB}$ ), with subsurface flow from forest and grassland ( $K_{fF}$  and  $K_{fG}$ ) parameterized to  
474 operate at intermediate timescales.

**Table 3.** Uniform prior parameter distributions of four models. **Note:**  $S_{r,max}$  and  $S_{tr,max}$  do not belong to the FLEX<sup>T</sup> model.

Models	Parameter	Explanation	Prior range
	$S_{i,max}$ (mm)	Storage capacity of interception reservoir	(0.1, 2)
	$S_{u,max}$ (mm)	Root zone storage capacity	(5, 300)
	$K_r$ (d)	<a href="#">Recession coefficient of fast response reservoir</a>	<a href="#">(1, 10)</a>
	$C_e$ (-)	Threshold controls actual evaporation and transpiration	(0, 1)
	$\beta$ (-)	Shape parameter of the tension water storage capacity curve	(0.1, 5)
FLEX <sup>L</sup>	$D$ (-)	Splitter between <del>surface</del> fast runoff and <del>groundwater</del> slow recharge	(0, 1)
		Time lag between storm and fast runoff generation	
FLEX <sup>D</sup>	$T_{lag}$ (-)	<del>fast-runoff-generation</del>	(0.8, 3)
		<del>fast-runoff-generation</del>	
FLEX <sup>T</sup>	$K_r$ (d)	<del>Recession coefficient of fast response reservoir</del>	<del>(1, 10)</del>
	$K_s$ (d)	Recession coefficient of slow response reservoir	(10, 200)
	$T_i$ (°C)	Threshold temperature to split snowfall and rainfall	(-2, 2)
	$T_m$ (°C)	Threshold temperature for melting	(-2, 2)
	$F_{dd}$ (mm(°Cd) <sup>-1</sup> )	Snow degree day factor	(1, 6)
	$P_L$ (mm/d)	<a href="#">Infiltration threshold for initiating Hortonian overland flow</a>	<a href="#">(5, 35)</a>



## 4.2 ~~Snow contribution~~ The ratio of snowmelt runoff to streamflow

This study ~~tracks~~ quantifies the ~~contribution ratio~~ of snowmelt runoff to streamflow ~~based on~~ using the FLEX<sup>T</sup> model. The model assumes that snowmelt and rainfall mix rapidly and completely upon entering the model's conceptual reservoirs, thereby altering its internal composition ratios. The composition ratio of the water exiting the reservoir is identical to that within the reservoir. ~~The contributions from snowmelt and rainfall represent portions of runoff generated at each time step, with some water remaining in the reservoir to participate in subsequent mixing, runoff generation, evaporation, and other hydrological processes (Liu et al., 2023)(Liu et al., 2023).~~ The method enables the tracking of ~~the contribution ratio~~ of snowmelt ~~to total~~ runoff ~~(C~~ to streamflow ( $f_{Q,snow}$ ) at each time step by the following equation:

$$C = \frac{Q_M}{Q} f_{Q,snow} = \frac{Q_M}{Q} = \frac{Q_{f,M} + Q_{s,M}}{Q}$$

(24)(26)

$$Q_{f,M} = \frac{\left(\frac{M}{P_{ef}+M}\right) S_f}{K_f} \frac{\left(\frac{M}{P_e}\right) S_f}{K_f}$$

(25)(27)

$$Q_{s,M} = \frac{\left(\frac{M}{P_{ef}+M}\right) S_s}{K_s} =$$

$$\frac{\left(\frac{M}{P_e}\right) S_s}{K_s}$$

(26)(28)

where  $Q$  is total runoff in the river channel;  $Q_M$  is snowmelt runoff in the river channel;  $Q_{f,M}$  is surface flow or subsurface storm flow generated by snowmelt;  $Q_{s,M}$  is groundwater flow generated by snowmelt.

## 4.3 Model calibration and uncertainty estimation

~~In~~ For the Bogd Uliastai river basin, the model was ~~pre-warmed~~ up using data from 2007; ~~the years, calibrated during 2008–2011 were used for calibration,~~ and validated during 2012–2015 ~~for validation.~~ In. For the Zavkhan Guulin river basin, 2000 was used as the warm-up year, with 2001–2010 selected for calibration and 2011–2020 for validation.

503

504 The MOSCEM-UA (Multi-objective Shuffled Complex Evolution Metropolis  
505 Algorithm) integrates multi-objective optimization and Bayesian uncertainty analysis,  
506 featuring global search capabilities that facilitate the generation of multiple Pareto  
507 optimal solutions and provide an assessment of uncertainty (~~Vrugt et al., 2003~~)(Vrugt  
508 et al., 2003). The MOSCEM-UA was run for the optimization of parameters, with  
509 40000 iterations for each of the four model structures. The model parameters and their  
510 prior ranges for calibration are listed in Table 3.

511

512 The Kling-Gupta Efficiency (KGE) and its logarithmic form (KGL) were used as  
513 objective functions to evaluate the simulation of daily discharge (~~Gupta et al.,~~  
514 2009)(Gupta et al., 2009). These two metrics were chosen because each emphasizes a  
515 different portion of the hydrograph: KGE is more sensitive to high-flow dynamics,  
516 while KGL better captures low-flow conditions. In this study, to accommodate  
517 minimization-based optimization algorithms, the runoff objective functions  $L_1$   
518 (Eq.2729) and  $L_2$  (Eq.2830) were formulated as one minus their respective efficiency  
519 metrics. The two objective functions were assigned equal weights during model  
520 calibration to ensure a balanced representation of both high- and low-flow regimes.

$$521 L_1 = 1 - KGE = \sqrt{(1 - \gamma)^2 + (1 - \alpha)^2 + (1 - \beta)^2}$$

522 (2729)

$$523 L_2 = 1 - KGL = \sqrt{(1 - \gamma_{log})^2 + (1 - \alpha_{log})^2 + (1 - \beta_{log})^2}$$

524 (2830)

525 where,  $\gamma$  is the correlation coefficient between simulated and observed flows, and  $\gamma_{log}$  is  
526 the correlation coefficient between their logarithmic values;  $\alpha$  is the ratio of the standard  
527 deviations of the simulated and observed flows, and  $\alpha_{log}$  is the ratio of the standard  
528 deviations of their logarithmic transformations;  $\beta$  is the ratio of the mean values of the  
529 simulated and observed flows, and  $\beta_{log}$  is the ratio of the mean values of their  
530 logarithmic transformations.

## 531 **5. Results and discussion**

## 532 **5.1 Model calibration and validation**

533 Fig.4 shows the performance of the four models during the calibration period. The  
534 Pareto-optimal front shifts progressively toward the origin, indicating that model  
535 structural modifications enhance the model's ability to capture basin runoff dynamics.  
536 The FLEX<sup>L</sup>-S model (KGE: 0.65 and 0.65, with the former representing the Bogd  
537 Uliastai river basin and the latter representing the Zavkhan Guulin river basin,  
538 hereinafter referred to as the same; KGL: 0.68 and 0.66) (Table 4) outperforms the  
539 baseline FLEX<sup>L</sup> model (KGE: 0.53 and 0.52; KGL: 0.62 and 0.48) (Table 4). This  
540 improvement highlights the importance of explicitly representing snow processes in  
541 cryospheric regions. Without accounting for snow accumulation and ablation, the  
542 model tends to overestimate ~~minor~~small peak flow events in winter, as shown in Fig.5,  
543 underscoring the critical role of snow dynamics in shaping hydrological responses.

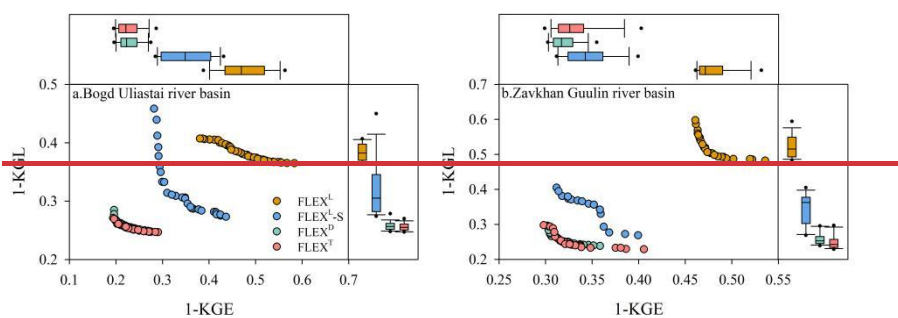
544

545 The FLEX<sup>D</sup> model (KGE: 0.77 and 0.68; KGL: 0.74 and 0.74) outperforms the FLEX<sup>L</sup>-  
546 S, with the distributed precipitation and temperature inputs significantly improving the  
547 simulation of peak flow. ~~Notably, FLEX<sup>D</sup> does not require a more complex model~~  
548 ~~structure or additional parameters compared to FLEX<sup>L</sup>-S. However, it allows each~~  
549 ~~hydrological response unit to maintain distinct storage states in the interception, snow,~~  
550 ~~and unsaturated reservoirs on any given day. This capability effectively overcomes a~~  
551 ~~key limitation of lumped models, which are unable to represent the spatial variability~~  
552 ~~of hydrological responses across heterogeneous landscapes. For hydrograph simulation,~~  
553 ~~FLEX<sup>T</sup> (KGE: 0.78 and 0.68; KGL: 0.75 and 0.75) performs comparably to FLEX<sup>D</sup>.~~  
554 ~~For hydrograph simulation, FLEX<sup>F</sup> (KGE: 0.77 and 0.67; KGL: 0.74 and 0.75)~~  
555 ~~performs comparably to FLEX<sup>D</sup>. This similarity in performance despite FLEX<sup>F</sup>'s~~  
556 ~~increased model complexity and more physically interpretable parameters may be~~  
557 ~~attributed to two main factors. First, both basins are dominated by grasslands, which~~  
558 ~~cover more than 80% of the area, resulting in low vegetation heterogeneity (Fig.3).~~  
559 ~~Second, vegetation characteristics—such as rooting depth and interception capacity—~~

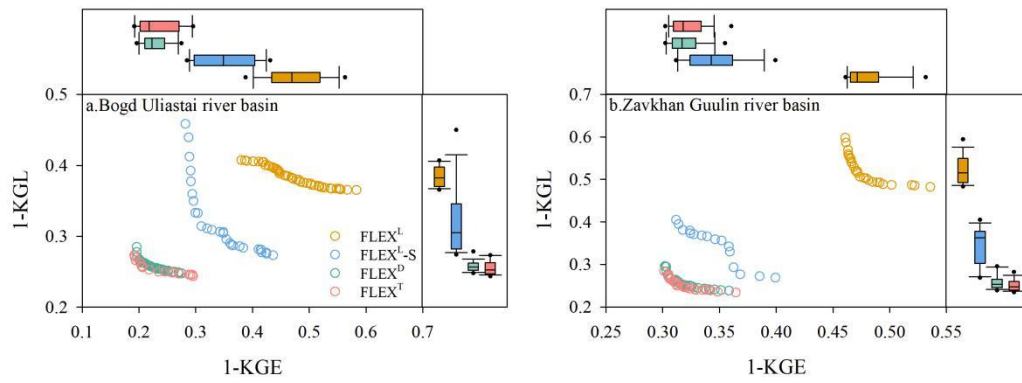
560 may already be implicitly represented by hydroclimatic and topographic variables  
561 (Antonelli et al., 2018; Roebroek et al., 2020), thereby diminishing the added value of  
562 explicitly incorporating vegetation information in this case.

563  
564 As shown in Fig.6, the lumped model employs a spatially uniform NDVI value, which  
565 cannot reflect intra-basin vegetation variability. Nevertheless, a strong correspondence  
566 is observed between elevation and NDVI, particularly in grassland-dominated regions.  
567 NDVI values across elevation bands closely match those of the corresponding grassland  
568 zones, suggesting that vegetation distribution is strongly aligned with topographic  
569 gradients. Although NDVI differs significantly between forested and bare land areas,  
570 these land cover types occupy only a small fraction of the basin and contribute  
571 negligibly to runoff generation. In this context, elevation can serve as a reliable proxy  
572 for vegetation structure, effectively embedding vegetation-related hydrological  
573 influence within the topographic representation. These findings support the notion that  
574 hydroclimatic and terrain-based variables may indirectly encode essential vegetation  
575 processes in distributed or semi-distributed models.

576  
577 Together, these results suggest that the limited vegetation heterogeneity in the study  
578 basins may constrain the potential performance gains of FLEX<sup>T</sup> over the simpler  
579 FLEX<sup>D</sup> model. Nonetheless, the strength of FLEX<sup>T</sup> lies in its explicit representation of  
580 distinct landscape units, enabling a more physically grounded simulation of  
581 hydrological processes and underlying mechanisms. Further research is warranted to  
582 evaluate the benefits of the landscape-based modeling approach in catchments with  
583 greater ecological and topographic complexity.



585



586

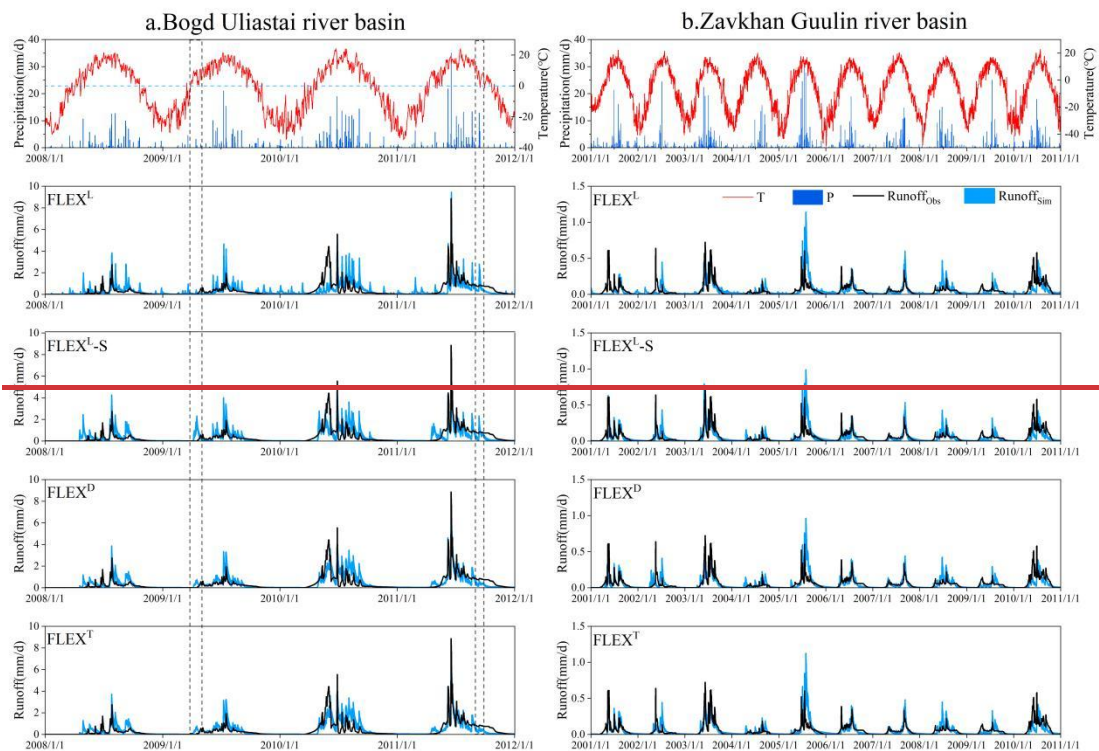
587 **Fig.4** Performance of the FLEX<sup>L</sup>, FLEX<sup>L-S</sup>, FLEX<sup>D</sup>, and FLEX<sup>T</sup> models during the calibration

588 modeperiod.

**Table 4** Comparison of simulation performance among different hydrological models in the **two** study catchments.

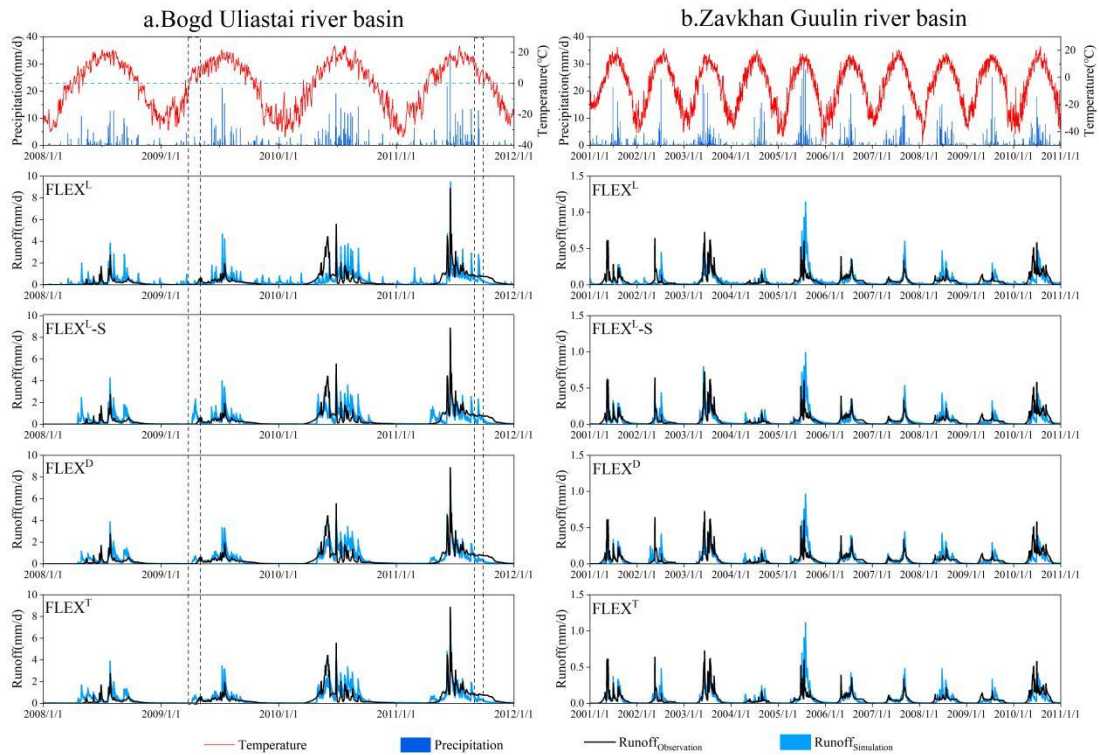
Basins	Evaluation indicators	Calibration						Validation			
		FLEX <sup>L</sup>	FLEX <sup>L-S</sup>	FLEX <sup>D</sup>	FLEX <sup>T</sup>	FLEX <sup>L</sup>	FLEX <sup>L-S</sup>	FLEX <sup>L-S</sup>	FLEX <sup>D</sup>	FLEX <sup>T</sup>	
Bogd Uliastai river basin	Max	0.62	0.72	0.80	0.81	0.58	0.63	0.62	0.63	0.63	
	Median	0.53	0.65	0.77	<del>0.7778</del>	0.39	0.47	0.56	<del>0.5759</del>		
	Min	0.42	0.56	0.73	<del>0.7470</del>	0.16	0.29	0.52	<del>0.5251</del>		
	Max	0.63	0.73	0.75	<del>0.7576</del>	0.67	0.76	0.80	<del>0.8081</del>		
	Median	0.62	0.68	0.74	<del>0.7475</del>	0.64	0.71	0.78	0.78		
	Min	0.59	0.54	0.72	0.73	0.61	0.61	0.75	0.75		
Zavkhan Guulin river basin	Max	0.54	0.69	0.70	0.70	0.41	0.59	0.62	<del>0.6463</del>		
	Median	0.52	0.65	0.68	<del>0.6768</del>	0.31	0.47	0.56	<del>0.5659</del>		
	Min	0.46	0.60	0.64	<del>0.5964</del>	0.13	0.28	0.41	<del>0.4052</del>		
	Max	0.52	0.73	0.76	0.77	0.60	0.73	0.74	<del>0.7674</del>		
	Median	0.48	0.66	0.74	0.75	0.56	0.66	0.72	0.73		
	Min	0.40	0.60	0.70	<del>0.7072</del>	0.47	0.61	0.70	<del>0.6971</del>		

591 Some interesting rain/snowmelt-runoff events also suggest that semi-distributed models  
592 (FLEX<sup>D</sup> and FLEX<sup>T</sup>) better capture basin hydrological processes. Two such events in  
593 the Bogd Uliastai river basin in April 2009 and September 2011 provide compelling  
594 evidence (Fig.5). ~~In On 14 April 2009, despite minimal precipitation, temperatures~~  
595 ~~exceeded the melting threshold, producing only a relatively insignificant peak flow. In~~  
596 ~~12 September 2011, despite a higher daily precipitation of 12.7 mm, no runoff peak was~~  
597 ~~observed within the basin. Lumped models failed to reproduce these dynamics~~  
598 ~~accurately, instead simulating much larger peak flows. This limitation arises because~~  
599 ~~lumped models do not account for elevation dependent variations in temperature and~~  
600 ~~precipitation type. When the average daily temperature exceeds the rain-snow~~  
601 ~~separation (snowmelt) threshold, lumped models treat all precipitation as rain~~  
602 ~~(snowmelt is assumed to occur uniformly across the entire basin). However, snowfall~~  
603 ~~may still occur at higher elevations, where temperatures are below the threshold,~~  
604 ~~resulting in limited snowmelt. Similarly, rainfall (and corresponding snowmelt) may~~  
605 ~~occur in lower elevations even when the basin average temperature falls below the~~  
606 ~~threshold.~~



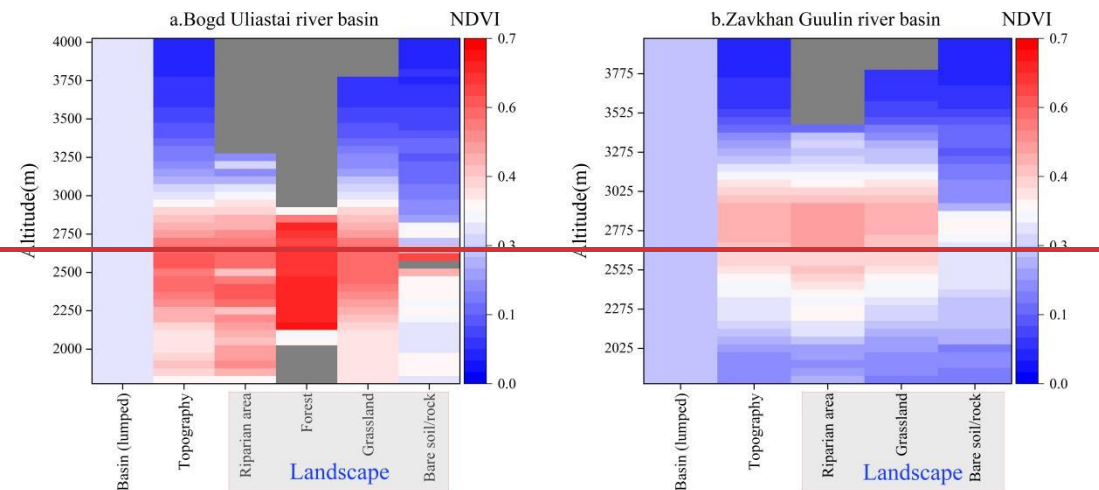
607

608



609

610 **Fig.5** The daily observed and simulated hydrographs of the FLEX<sup>L</sup>, FLEX<sup>L</sup>-S, FLEX<sup>D</sup>, and FLEX<sup>T</sup>  
 611 models in the calibration period. The dashed boxes represent the rainfall/snowfall-runoff events ~~in~~  
 612 on 14 April 2009 and 12 September 2011 in the Bogd Uliastai river basin.



613

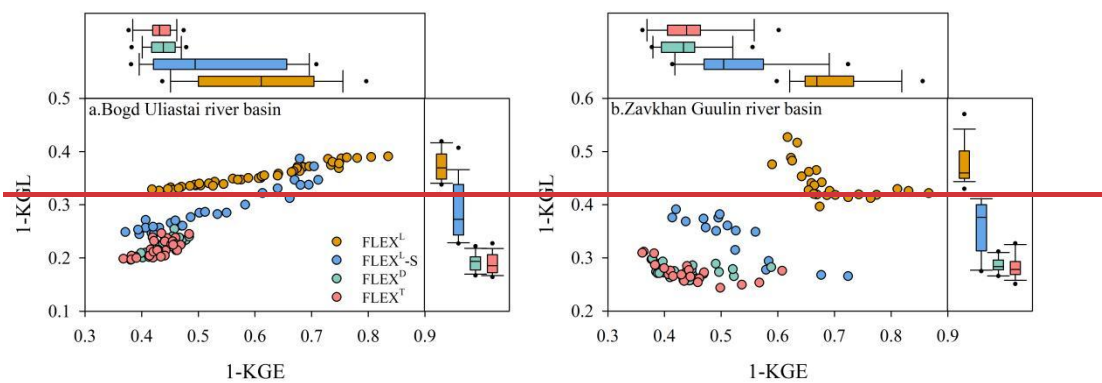
614 **Fig.6** Multi-year average NDVI variation across landscapes and its relationship with elevation in  
 615 two study basins.

616

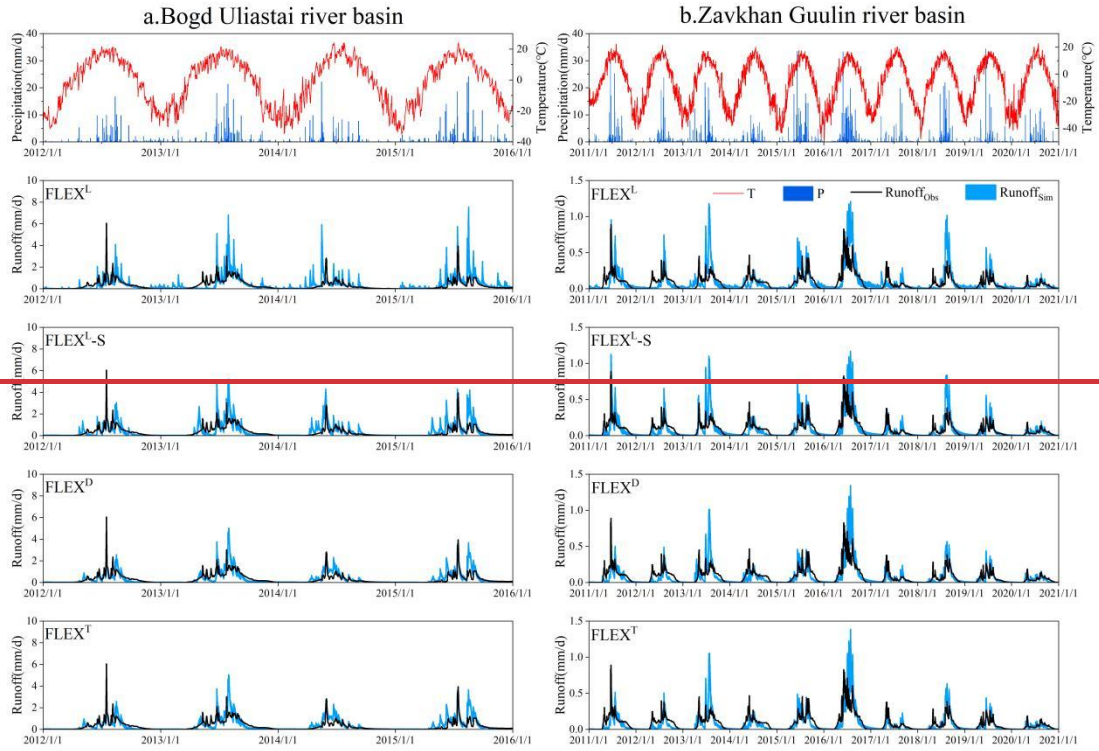
617 The performance and results of the four models during the validation period are shown  
 618 in Figs. 6 and 7 ~~and 8~~. The results confirm the stepwise improvement in model

619 performance, as evidenced by the points corresponding to different model structures  
620 progressively shifting toward the origin. With the gradual optimization of model  
621 structure, the model's fitness has significantly improved. Unlike during calibration, the  
622 points in the validation period do not maintain the arc shape (Fig.4). ~~This discrepancy  
623 is attributed to errors present in both the model and the data, the estimation of which  
624 remains a challenging task (Fenicia et al., 2008b).~~

625  
626 ~~In summary, a model's ability to reproduce basin-scale hydrological responses is  
627 governed not by the complexity of its structure or the sheer number of parameters, but  
628 by the relevance and accuracy of the hydrological processes it represents, and their  
629 influence on catchment-scale dynamics.~~



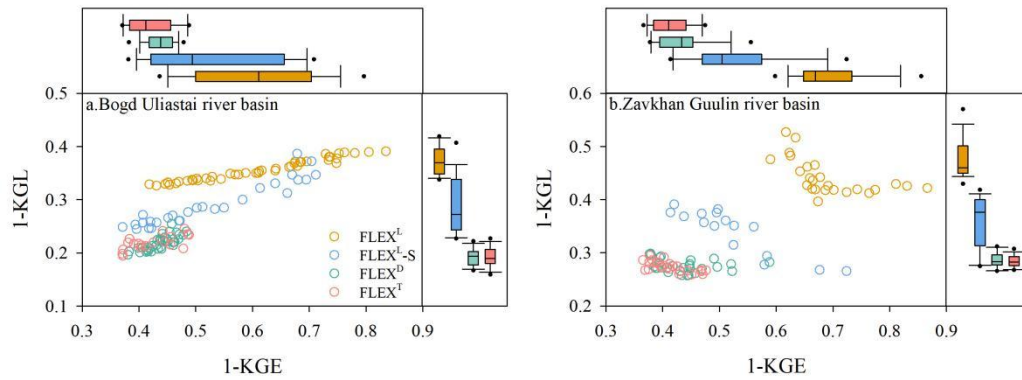
630  
631 ~~Fig.7 Performance of the FLEX<sup>L</sup>, FLEX<sup>L-S</sup>, FLEX<sup>D</sup>, and FLEX<sup>T</sup> models in validation mode.~~



632

633

**Fig.8**

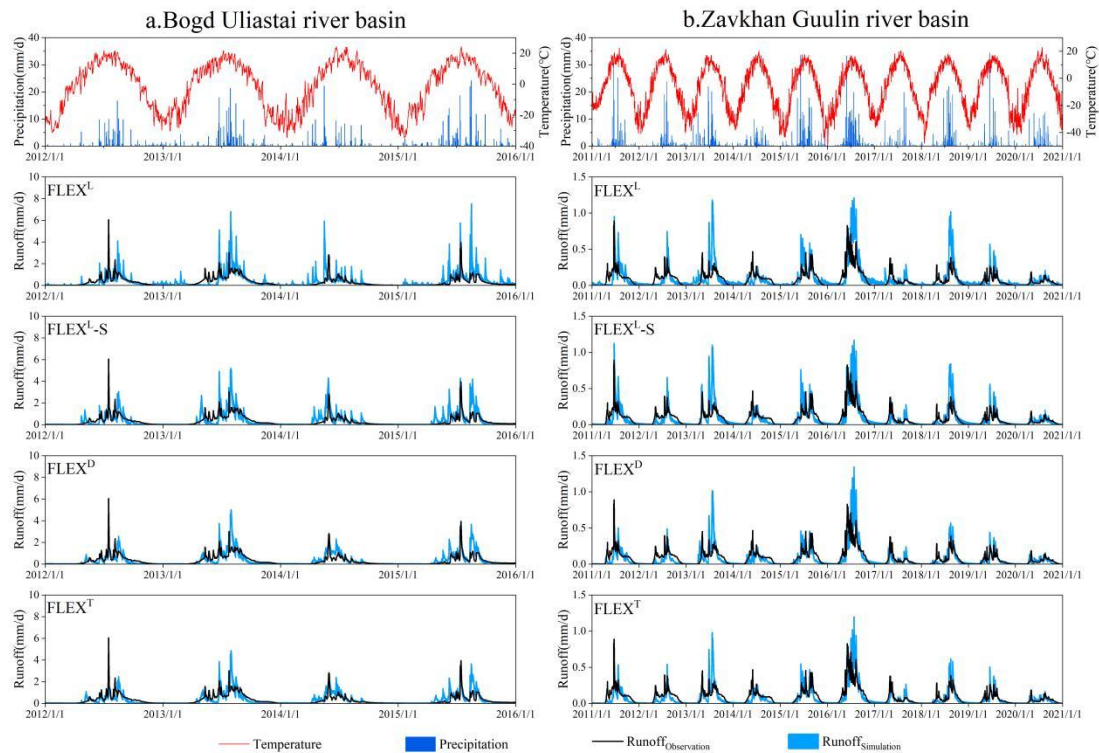


634

635

**Fig.6** Performance of the FLEX<sup>L</sup>, FLEX<sup>L-S</sup>, FLEX<sup>D</sup>, and FLEX<sup>T</sup> models in validation mode.

636



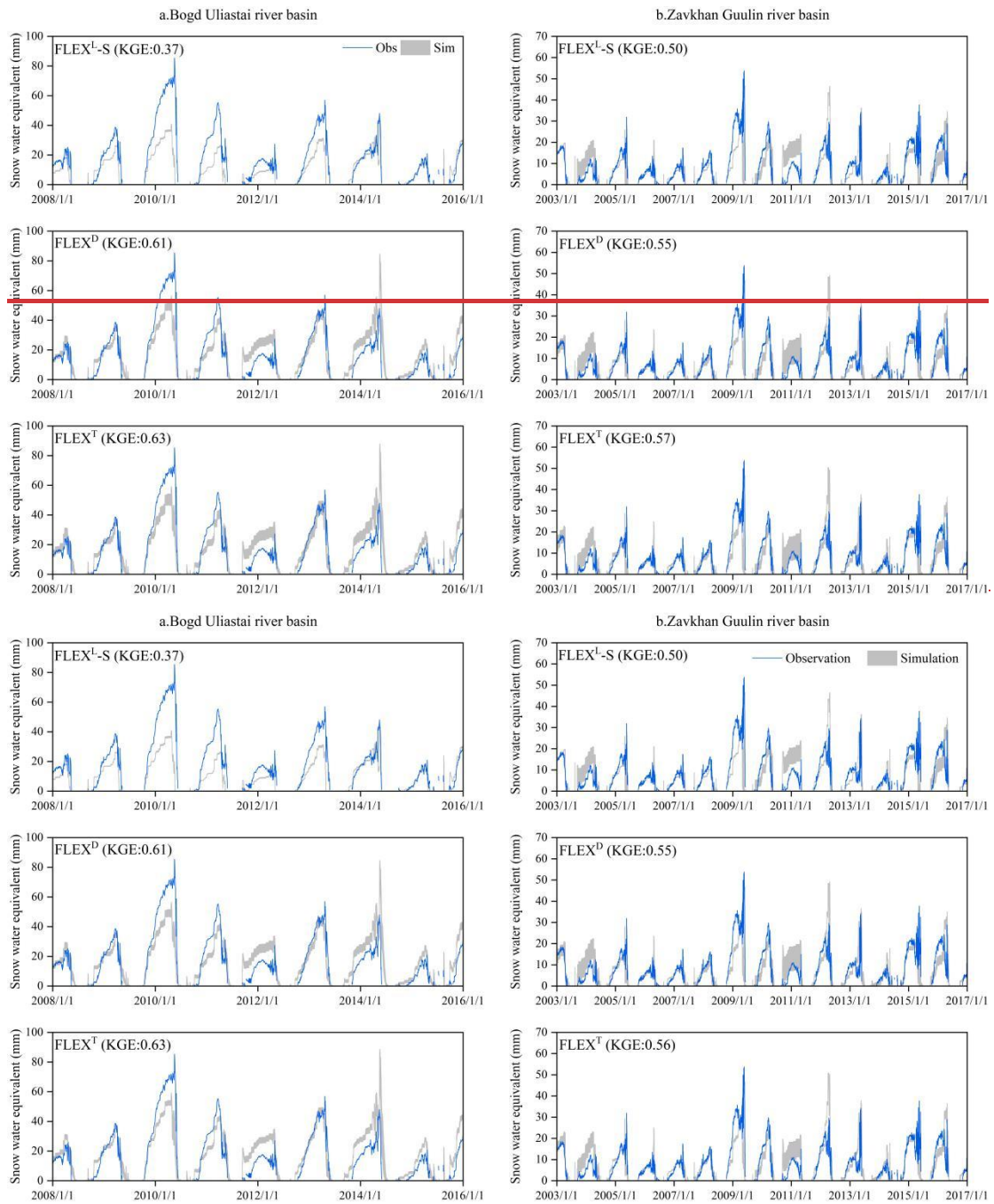
637

638 **Fig.7** The daily observed and simulated hydrographs of the FLEX<sup>L</sup>, FLEX<sup>L</sup>-S, FLEX<sup>D</sup>, and FLEX<sup>T</sup>  
 639 models in the validation period.

640

## 641 5.2 Model test by snowpack dynamics

642 Snow water equivalent is a crucial indicator of snowmelt dynamics and plays an  
 643 essential role in hydrological ~~modeling~~ modelling, serving as an additional metric for  
 644 evaluating model performance and realism (Fig.98). In the Bogd Uliastai river basin,  
 645 the FLEX<sup>D</sup> and FLEX<sup>T</sup> models achieved KGE values of 0.61 and 0.63, respectively, for  
 646 SWE simulation, indicating their ability to capture seasonal patterns and interannual  
 647 variability, particularly peak values during winter and spring. The FLEX<sup>T</sup> model, which  
 648 incorporates vegetation effects, further improved SWE simulation accuracy and  
 649 enhanced responsiveness to hydrological processes. In contrast, the FLEX<sup>L</sup>-S model  
 650 yielded a KGE of only 0.37, reflecting its limitations in capturing snowpack dynamics  
 651 within the basin. ~~Lumped models typically simplify the spatial heterogeneity of factors~~  
 652 ~~such as terrain and vegetation, limiting their ability to capture local scale features and~~  
 653 ~~consequently reducing accuracy in complex environments (Bormann et al., 2009).~~



654

655

656 **Fig.98** The observed and simulated daily snow water equivalent of the FLEX<sup>L</sup>-S, FLEX<sup>D</sup>, and  
 657 FLEX<sup>T</sup> models.

658

659 In the Zavkhan Guulin river basin, the FLEX<sup>L</sup>-S model demonstrated relatively stable  
 660 performance, achieving a KGE of 0.50. Although lumped models struggle to capture  
 661 spatial heterogeneity, they effectively reflect seasonal precipitation and snowmelt  
 662 trends. FLEX<sup>D</sup> and FLEX<sup>T</sup> achieved KGE values of 0.55 and 0.57, respectively, showed  
 663 slight improvements. Model effectiveness remains strongly influenced by basin-

664 specific climatic and landscape features—such as steep slopes, variable precipitation  
665 patterns, heterogeneous vegetation, and local climate fluctuations—all of which  
666 complicate accurate simulation of local-scale hydrological responses (Greco et al., 2023;  
667 Nippgen et al., 2011). These challenges are further amplified in data-scarce, cold  
668 regions, where disentangling the interactions among these factors is particularly  
669 difficult (Chen et al., 2017). While current models provide valuable insights, further  
670 refinement and validation are necessary to better capture dynamic local processes and  
671 microclimatic effects. 56, respectively, showed slight improvements. Overall, the semi-  
672 distributed model exhibited consistently higher SWE simulation skill across both basins.

### 674 5.3 Model parameters composition

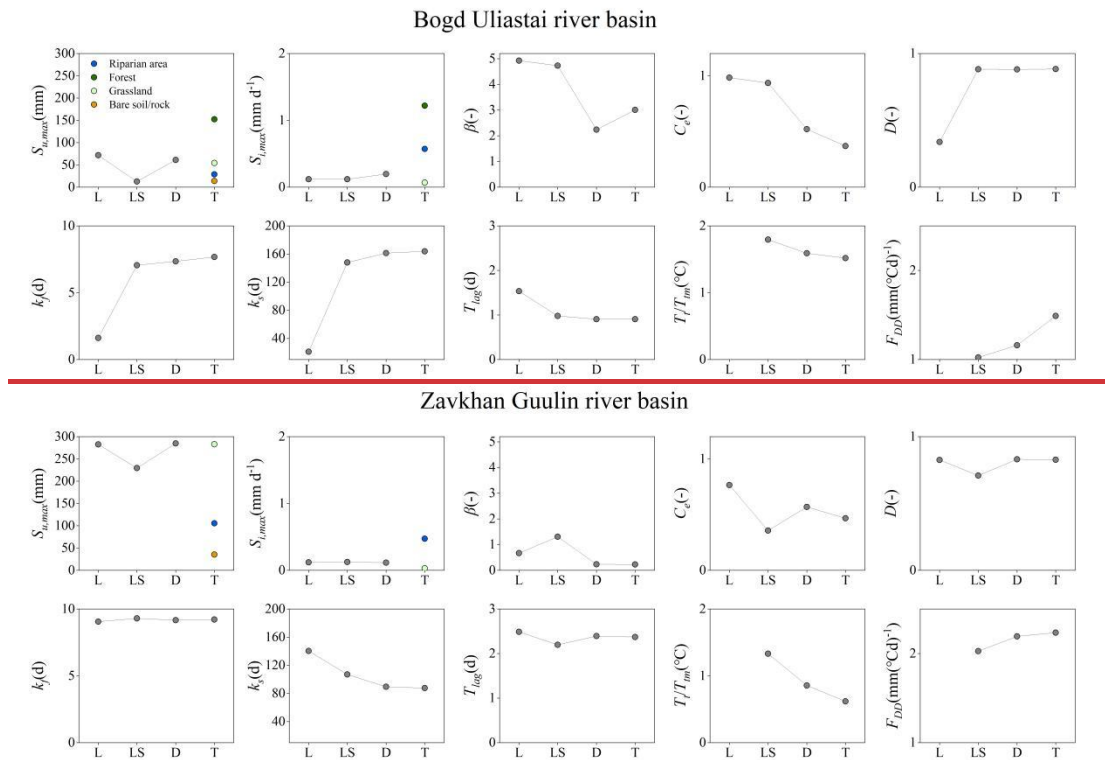
675 A key feature of the stepwise modelling framework is the progressive refinement of  
676 parameterization towards greater physical realism. As shown in Fig.10,9 shows that  
677 model parameters exhibit distinct sensitivity across different structural configurations  
678 within the stepwise modelling framework. In models that do not account for vegetation  
679 effects, single parameter values are used to approximate basin-average hydrological  
680 behavior. By contrast, the, whereas FLEX<sup>T</sup> model incorporates landscape-specific  
681 hydrological response characteristics, resulting in produces spatially differentiated  
682 parameter values that better reflect underlying process heterogeneity across landscape  
683 units.

684  
685 Forest, characterized by dense canopies, exhibit a higher value of  $S_{i,maxF}$  (1.22 mm),  
686 effectively regulating water distribution during the initial stages of rainfall events  
687 (Wang et al., 2021). In comparison,  $S_{i,maxG}$  (0.07 mm and 0.03 mm for the Bogd Uliastai  
688 and Zavkhan-Guulin river basins, respectively) and  $S_{i,maxR}$  (0.57 mm and 0.47 mm) are  
689 lower. The riparian area, however, shows greater interception capacity than grassland,  
690 likely due to denser or more abundant vegetation cover (Gao et al., 2014). Bare soil/rock  
691 surfaces lack interception capacity altogether, with rainfall either infiltrating directly  
692 into the ground or rapidly generating surface runoff along slopes.—

693

694 For root zone storage capacity,  $S_{u,maxF}$  is 150 mm, consistent with the findings of Wang-  
695 Erlandsson et al. (Wang Erlandsson et al., 2016). Notable differences are observed in  
696  $S_{u,maxG}$  (54 mm and 283 mm) and  $S_{u,maxR}$  (29 mm and 105 mm) under varying climatic  
697 conditions.  $S_{u,maxB}$  (14 mm and 33 mm) exhibits the lowest values due to the absence of  
698 vegetation cover and limited soil structure development (He et al., 2024).

699 The differences in interception and root zone storage capacity across landscapes  
700 between the two basins are primarily attributed to the more arid conditions in the  
701 Zavkhan Guulin river basin. This basin is characterized by sparse vegetation (reflected  
702 in lower  $S_{i,max}$ ), higher evaporation losses (as suggested by greater  $S_{u,max}$ ), and a low  
703 runoff coefficient of only 0.15.

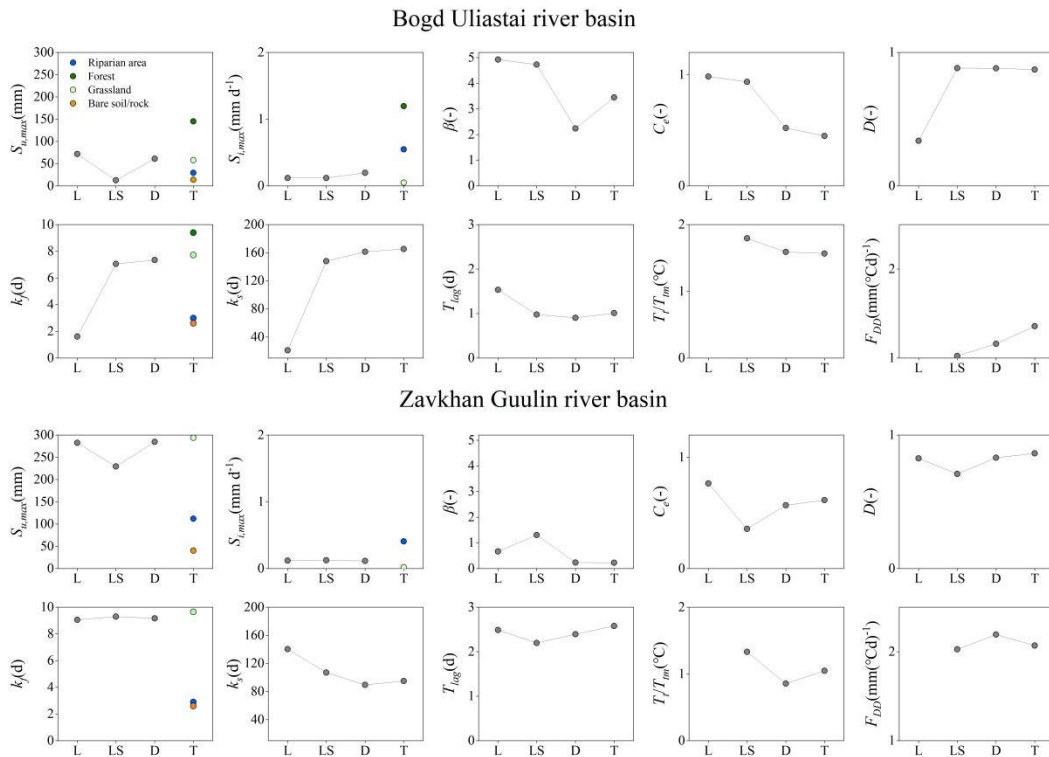


704

705 Interception capacity ( $S_{i,max}$ ) and root zone storage capacity ( $S_{u,max}$ ) vary across  
706 landscapes. In the Bogd Uliastai river basin, forest (present only in this basin) shows  
707 the highest  $S_{i,max}$  (1.19 mm), followed by riparian area (0.55 mm) and grassland (0.05  
708 mm), while bare soil/rock has no interception storage.  $S_{u,max}$  decreases from forest (145  
709 mm) to grassland (54 mm), riparian area (29 mm), and bare soil/rock (14 mm). By  
710 comparison, in the Zavkhan Guulin river basin,  $S_{i,max}$  is lower (grassland: 0.02 mm;

711 riparian area: 0.41 mm), whereas  $S_{u,max}$  is higher (grassland: 283 mm; riparian area: 105  
 712 mm; bare soil/rock: 33 mm), reflecting the more arid conditions and associated  
 713 hydrological characteristics.

714 —  
 715 The recession coefficient of the fast response reservoir ( $K_f$ ) reflects runoff dynamics  
 716 and storage across landscapes. In the Bogd Uliastai river basin, forest has the largest  $K_f$   
 717 (9.4 d), followed by grassland (7.7 d), while riparian areas (3.0 d) and bare soil/rock  
 718 (2.6 d) have the smallest  $K_f$ , indicating faster runoff. In the Zavkhan Guulin river basin,  
 719  $K_f$  shows a similar pattern, with grassland (9.7 d), riparian areas (2.9 d), and bare  
 720 soil/rock (2.5 d). The low  $K_f$  in bare soil/rock reflects Hortonian overland flow, whereas  
 721 runoff in riparian areas is mainly governed by saturation overland flow.



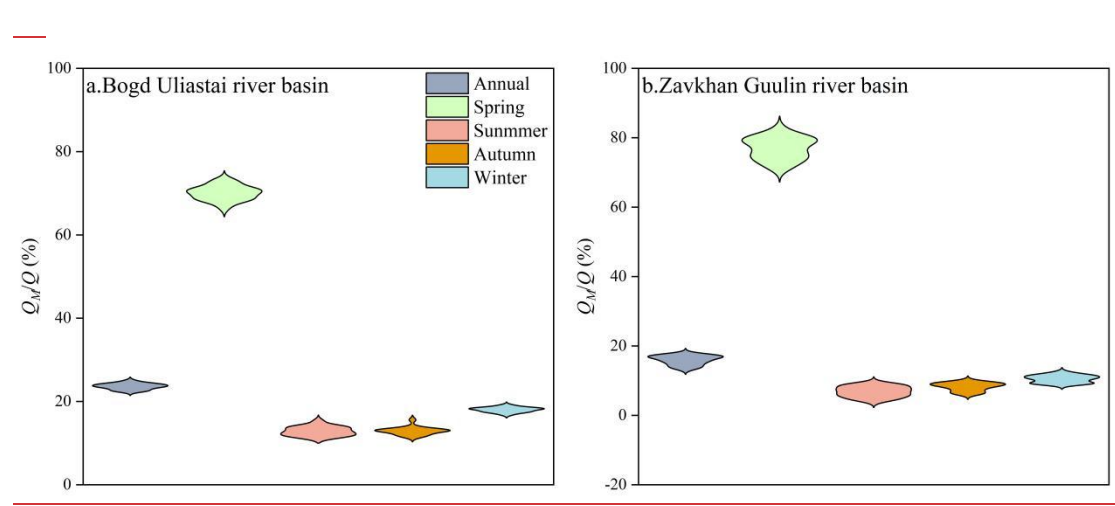
722  
 723 **Fig.109** The changes of averaged behavioral parameters of the FLEX<sup>L</sup>, FLEX<sup>L-S</sup>, FLEX<sup>D</sup>, and  
 724 FLEX<sup>T</sup> models.

725  
 726 Other parameters are also refined alongside improvements in the model structure. The  
 727 parameter  $D$ , which partitions generated runoff between fast and slow response  
 728 reservoirs, tends to be close to 1—indicating that most runoff is routed to the fast

729 reservoir. ~~This aligns with the observed runoff generation mechanisms in the study~~  
 730 ~~basins, which are primarily driven by intense rainfall events.~~ Parameters related to  
 731 energy processes, such as the  $T_{im}$  and  $F_{dd}$ , exhibit a clear compensatory relationship: a  
 732 higher  $T_{im}$  is typically associated with a lower  $F_{dd}$ , and vice versa. ~~This reflects model~~  
 733 ~~calibration trade-offs aimed at maintaining energy balance. Future work should~~  
 734 ~~incorporate field observations to better quantify parameter heterogeneity across~~  
 735 ~~different landscape units. Such efforts would enhance both the physical interpretability~~  
 736 ~~and predictive robustness of the model.~~

#### 738 **5.4 Snow contribution The ratio of snowmelt runoff to streamflow**

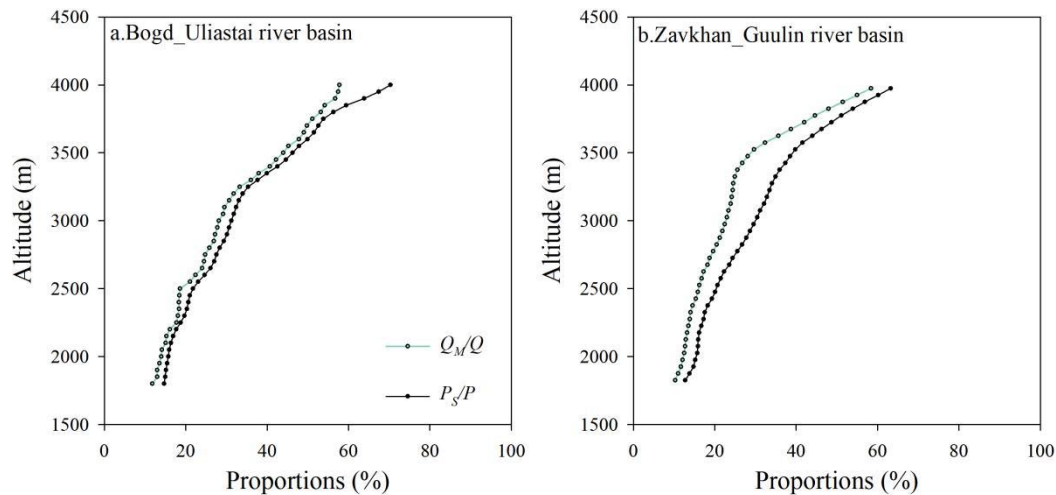
739 Fig.11 shows the annual and seasonal ~~contributions ratios~~ of snowmelt runoff  
 740 streamflow in the Bogd Uliastai and Zavkhan Guulin river basins, as  
 741 ~~determined simulated~~ by the FLEX<sup>T</sup> model. On an annual scale, snowmelt  
 742 ~~contributes runoff accounts for~~ 23.56%±0.7% and 15.9%±1.3% and 14.7%±1.6% to of  
 743 streamflow in the Bogd Uliastai and Zavkhan Guulin river basins, respectively.  
 744 Seasonally, snowmelt plays a dominant role in sustaining spring flows, with snowmelt  
 745 runoff accounting for 70.1%±1.7% and 76.9%±3.2% of streamflow in the two basins,  
 746 while its contribution is considerably lower in other seasons.



748  
 749 **Fig.10** The ratio of snowmelt runoff to streamflow based on the FLEX<sup>T</sup> model.

750  
 751 Fig.11 shows the snowfall-to-precipitation ratio ( $P_s/P$ ) and the ratio of snowmelt runoff

752 to streamflow ( $Q_M/Q$ ) across different elevations. The  $P_s/P$  increases with elevation  
753 ranging from 14.7% to 70.3% in the Bogd Uliastai river basin and from 12.7% to 63.2%  
754 in the Zavkhan Guulin river basin. Consistent with this pattern, the  $Q_M/Q$  also increases  
755 with elevation, from 11.8% to 57.8% and from 10.3% to 58.4% in the two basins,  
756 respectively. Overall, higher  $P_s/P$  are associated with higher  $Q_M/Q$  across elevations.



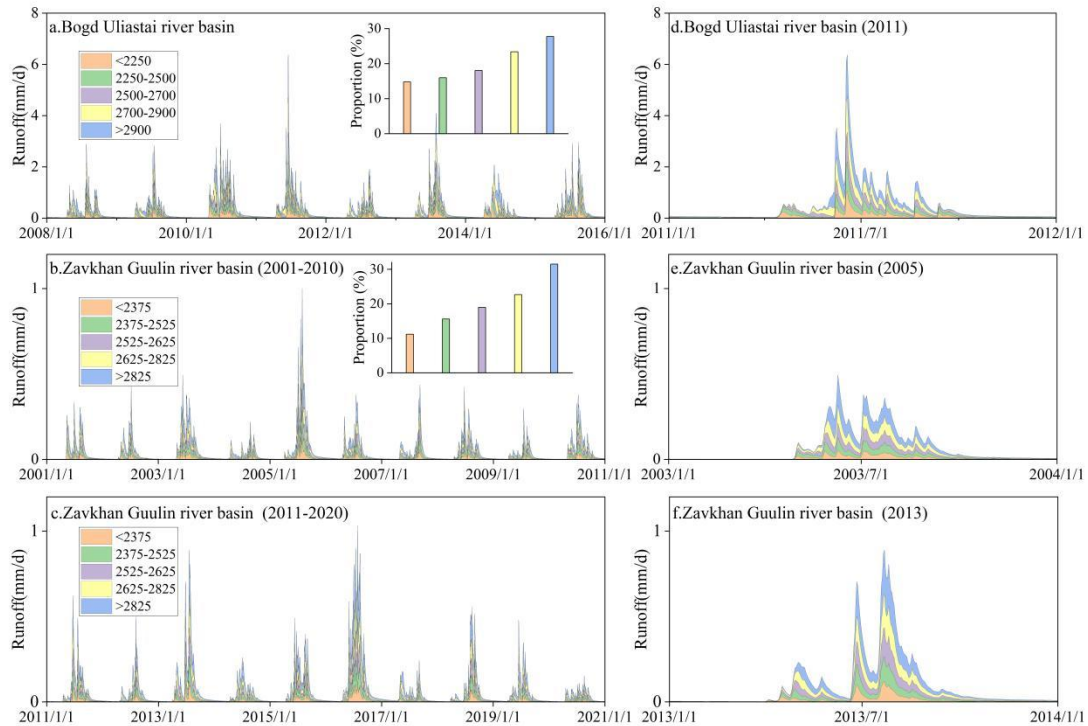
758 **Fig.11** The ratio of snowmelt runoff to streamflow and the snowfall-to-precipitation ratio at different  
759 elevations based on FLEX<sup>T</sup> model.

## 762 **5.5 Runoff generation at different elevations and across landscapes**

763 Fig.12 shows significant differences in runoff contributions across 5 equal area  
764 elevation bands. In the Bogd Uliastai and Zavkhan Guulin river basins, high elevation  
765 areas (above 2900 m in the Bogd Uliastai basin and 2825 m in the Zavkhan Guulin  
766 basin) play a dominant role in runoff generation, contributing approximately 30% of  
767 total basin runoff. This dominance is primarily attributed to orographic effect, which  
768 increase precipitation and enhance the proportion of snowmelt-derived runoff (Fig.11).  
769 In contrast, low elevation areas rely primarily on rainfall-induced runoff, while its  
770 contribution is considerably lower in other seasons. Although direct observational data  
771 (e.g., stable water isotopes) for quantifying snowmelt contributions are unavailable in  
772 this study, previous research provides indirect support. For example, Wu et al. (Wu et  
773 al., 2021) Due to limited precipitation and higher evaporative losses, their contributions

774 to total runoff are comparatively smaller, with the lowest elevation band accounting for  
775 only about 15% of basin runoff.

776 —



777

778 **Fig.12** Runoff contribution from 5 equal area elevation bands (each representing 20% of the total  
779 catchment area) based on FLEX<sup>T</sup> model.

780

781 Different landscape units also exhibit differences in their contributions to runoff (Fig.  
782 13). Grasslands occupy the largest portion of both basins (82.8% and 85.4% in the Bogd  
783 Uliastai and Zavkhan Guulin river basins, respectively) and contribute correspondingly  
784 high shares of total runoff (80.0% and 82.0%). Forested areas, found only in the Bogd  
785 Uliastai basin, account for 4.7% of the basin area but contribute only 2.9% of the total  
786 runoff. Riparian areas occupy a relatively small fraction of the two basins (10.3% and  
787 13.0%) but contribute a comparable or higher proportion of runoff (12.8% and 14.7%).  
788 Bare soil/rock areas generate a relatively high runoff contribution per unit area;  
789 however, their limited spatial extent (2.2% and 1.6%) constrains their total contribution  
790 to streamflow (4.3% and 3.3%).

791 —

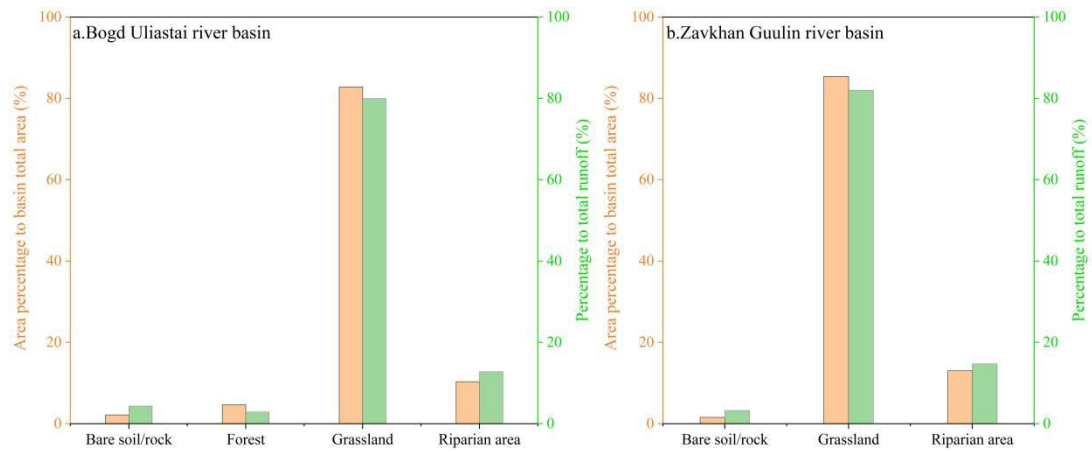


**Fig.13** Runoff contribution from different landscapes based on FLEX<sup>T</sup> model.

## **6. Discussion**

### **6.1 The stepwise modelling framework improves the simulation of hydrological processes in cold regions**

Accurately representing dominant hydrological processes and spatial heterogeneity is essential for simulating runoff dynamics in cold regions. The enhanced performance of FLEX<sup>L</sup>-S relative to the FLEX<sup>L</sup> model underscores the necessity of explicitly representing snow accumulation and melt, which are integral to runoff generation in cryospheric environments. Without such representation, winter runoff responses tend to be systematically mischaracterized.

The better performance of the distributed FLEX<sup>D</sup> model highlights the importance of elevation-dependent variability in temperature and precipitation (Fenicia et al., 2008b). By maintaining distinct storage states across hydrological response units, FLEX<sup>D</sup> captures spatial contrasts in precipitation phase and melt timing that lumped models fail to resolve, particularly during rain–snow transition events (Bormann et al., 2009).

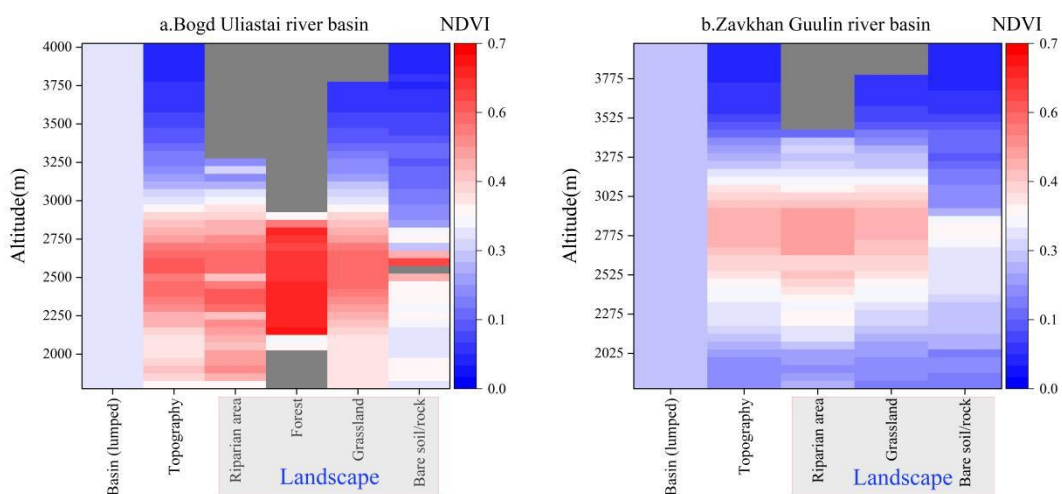
FLEX<sup>T</sup> systematically integrates topography, vegetation, and hydrological processes through the explicit representation of hydrological response units, thereby enhancing the physical consistency of the model structure and the interpretability of its parameters

814 (Savenije, 2010). Under the basin conditions considered in this study, FLEX<sup>T</sup> exhibits  
815 a high degree of consistency with FLEX<sup>D</sup> in simulating both runoff and snowpack  
816 dynamics. Although process-based discretization approaches have been shown to  
817 improve basin-scale hydrological simulations in heterogeneous cold region basins—  
818 such as the Heihe (Gao et al., 2014) and Yigong Zangbu river basins (Gao et al.,  
819 2020)—when topographic and land-cover variability are explicitly represented, the  
820 magnitude of these benefits appears to depend strongly on the degree of landscape  
821 heterogeneity.

822

823 In the studied basins, vegetation heterogeneity is limited, with grasslands covering  
824 more than 80% of the area (Fig.13), which substantially reduces contrasts in vegetation  
825 properties across the landscape. Although the lumped model applies a spatially uniform  
826 NDVI and therefore cannot explicitly resolve intra-basin vegetation variability, NDVI  
827 exhibits a strong correspondence with elevation, particularly in grassland-dominated  
828 regions. NDVI values across elevation bands closely resemble those of the  
829 corresponding grassland zones, indicating that vegetation distribution is largely  
830 structured by topographic gradients. While forested and bare land areas display distinct  
831 NDVI signatures, they occupy only a minor fraction of the basin and exert a limited  
832 influence on overall runoff generation (Fig.14).

833



834

835 Fig.14 Multi-year average NDVI variation across landscapes and its relationship with elevation in  
836 two study basins.

837  
838 Under these conditions, key vegetation-related hydrological attributes—such as root  
839 zone storage and interception capacity—can be effectively represented through  
840 hydroclimatic conditions and topographic gradients (Antonelli et al., 2018; Roebroek  
841 et al., 2020), allowing elevation to function, to some extent, as a proxy for vegetation  
842 structure. Consequently, the comparable performance of FLEX<sup>T</sup> and FLEX<sup>D</sup> in  
843 simulating runoff and snowpack processes primarily reflects the constraining influence  
844 of landscape structure in the studied basins, rather than differences in model design.  
845 Within this stepwise modelling framework, FLEX<sup>T</sup> employs a more physically  
846 grounded parameterization scheme and therefore offers a flexible and extensible  
847 platform for diagnosing hydrological processes in cold mountainous regions. This  
848 suggests a particular advantage for exploring hydrological responses to vegetation and  
849 climate change in basins with higher ecological or topographic complexity.

## 850 851 6.2 Process-based tracking of the ratio of snowmelt runoff to 852 streamflow

853 Although direct observational data (e.g., stable water isotopes) for quantifying the ratio  
854 of snowmelt runoff to streamflow are unavailable in this study, previous research  
855 provides indirect support. Wu et al. (2021) applied a similar snowmelt tracking method  
856 in the Altai Mountain and reported that snowmelt accounted for 29.3% of annual  
857 streamflow. This result exceeds those observed in our study, largely due to regional  
858 differences in snowfall. In the Kayiertes river basin of the Altai Mountain, annual  
859 average precipitation for one hydrological year (September to August) was 409.8 mm  
860 from 2011 to 2015 (observed at the Kuwei snow station), with snowfall from November  
861 to March comprising about 31% of that annual precipitation (Zhang et al., 2017)(Zhang  
862 et al., 2017). In contrast, annual precipitation in the Bogd Uliastai and Zavkhan Guulin

863 basins does not exceed 200 mm, and snowfall represents less than 15% of the total  
864 observed precipitation.

865

866 This study also compared model-based snowmelt tracking with traditional indirect  
867 methods, which estimate ~~the ratio of snowmelt contributions runoff to streamflow~~ by  
868 calculating the ratio of snowfall or snowmelt to runoff over a given period (~~Barnett et  
869 al., 2005; Immerzeel et al., 2010~~)(Barnett et al., 2005; Immerzeel et al., 2010). While  
870 ~~these indirect approaches are~~ computationally ~~simple and data~~-efficient, ~~these methods~~  
871 ~~and require limited data, they implicitly~~ assume that all meltwater ~~directly contributes is~~  
872 ~~instantaneously converted~~ to runoff, neglecting interactions with rainfall and losses due  
873 to infiltration, evaporation, and subsurface storage— (Li et al., 2017).

874

875 Using the traditional indirect approach, we calculated ~~the~~ snowmelt-to-runoff ratios ~~to~~  
876 ~~be 38.8%±2.0 of 41.3%±1.6% and 144.4%±20.1~~ 153%±15.5% in the two basins,  
877 respectively. These estimates are ~~significantly~~ substantially higher than those obtained  
878 ~~via from~~ model-based snowmelt tracking, with some values ~~even~~ exceeding 100%,  
879 indicating physical implausibility. This discrepancy highlights the methodological  
880 limitations and scientific inadequacies of traditional ~~methods. approaches.~~

881

882 The overestimation likely inherent in traditional methods arises from ~~the~~ their failure to  
883 ~~account for spatially disconnected snowmelt—specifically, represent~~ snowmelt that  
884 infiltrates into the ~~root zone and is subsequently soil profile, percolates to deeper layers,~~  
885 ~~or is~~ lost through evaporation-, thereby reducing the fraction of meltwater reaching the  
886 channel (Liu et al., 2023)(Liu et al., 2023), particularly in the arid Zavkhan Guulin river  
887 basin. These findings underscore the importance of using physically based models to  
888 trace water source pathways, particularly in data-scarce and hydrologically complex  
889 regions.

890 —

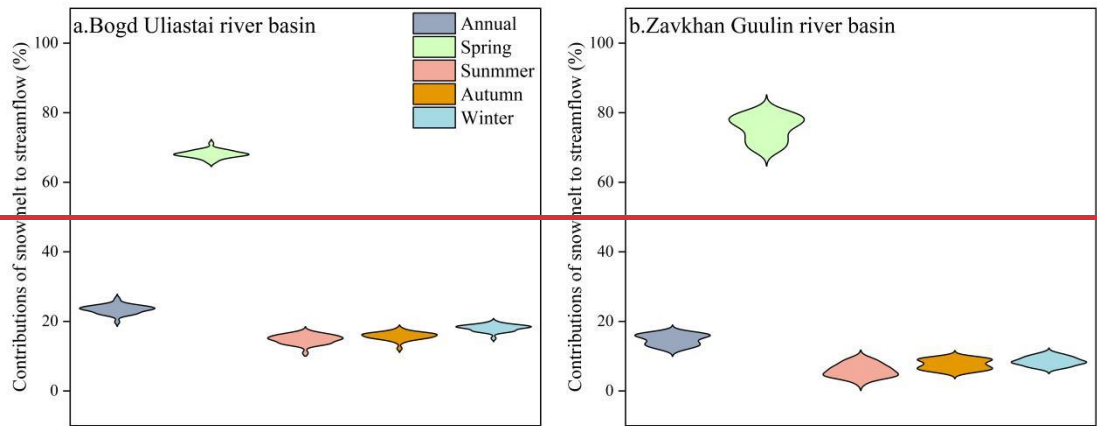


**Fig.11** Contributions of snowmelt to streamflow ( $Q_m/Q$ ) based on the FLEX<sup>T</sup> model.

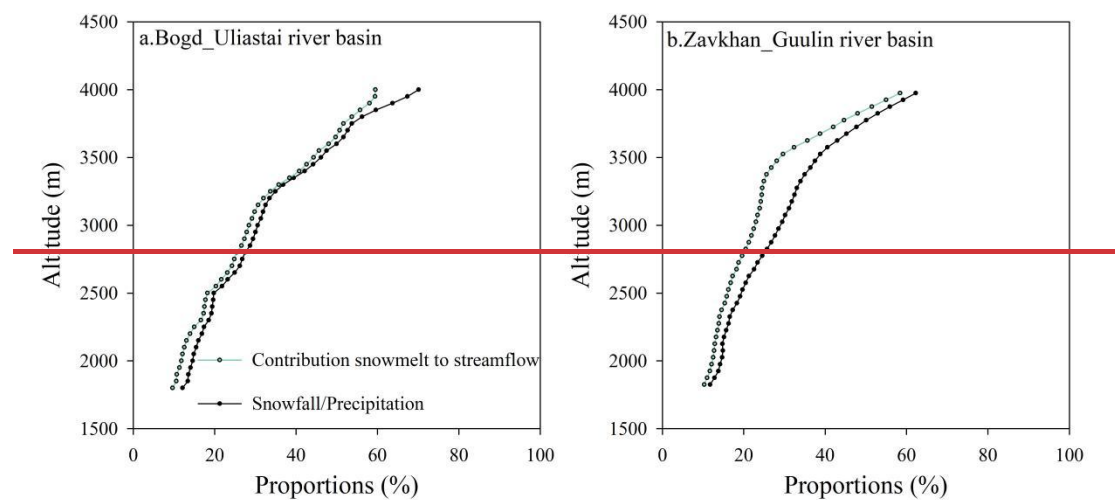
Fig.12 shows the snowmelt contribution to streamflow and the snowfall/precipitation ratio ( $P_s/P$ ) across different elevations. The results indicate that the  $P_s/P$  increases significantly attributable to lower temperatures at higher altitudes that favor snowfall. Correspondingly, the contribution of snowmelt to streamflow also increases with elevation, directly linked to greater snow storage in high elevation areas, which providing a sustained water source for rivers (Sprenger et al., 2024). The finding underscores the decisive influence of snowmelt on streamflow in mountainous regions. With rising temperatures driven by climate change, low elevation areas may see more precipitation as rain, reducing snowpack, while accelerated snowmelt at higher elevations could increase the variability and instability of meltwater runoff (Kraaijenbrink et al., 2021; Li et al., 2017).

Although the two basins share similar elevation and temperature regimes, their contrasting hydrological responses primarily reflect differences in climate and vegetation cover. The Bogd Uliastai river basin, dominated by mountainous grasslands, exhibits higher vegetation density (basin average NDVI: 0.31; grassland NDVI: 0.34), whereas the Zavkhan Guulin river basin, situated in a semi-arid region, shows lower vegetation cover (basin average NDVI: 0.26; grassland NDVI: 0.28) (Fig.6).

These vegetation differences influence snowmelt runoff efficiency. In Bogd Uliastai

914 ~~river basin, the snowmelt contribution to streamflow closely matches the snowfall to~~  
 915 ~~precipitation ratio, indicating limited losses and effective runoff generation. By contrast,~~  
 916 ~~Zavkhan Guulin river basin experiences greater hydrological losses—primarily due to~~  
 917 ~~infiltration and evaporation—which cause snowmelt contributions to fall below the~~  
 918 ~~snowfall input, especially at higher elevations (Litaor et al., 2008).~~

919  
 920 ~~Sparser vegetation and drier soils in Zavkhan Guulin river basin further enhance soil~~  
 921 ~~moisture retention, delaying runoff initiation and reducing the proportion of meltwater~~  
 922 ~~reaching the stream. This comparison highlights how subtle variations in vegetation~~  
 923 ~~structure, captured by NDVI, modulate hydrological partitioning and runoff efficiency~~  
 924 ~~across cold alpine landscapes (Zhong et al., 2021).~~



926  
 927 **Fig.12** Contributions of snowmelt to streamflow ( $Q_M/Q$ ) and snowfall/precipitation ratio ( $P_s/P$ ) at  
 928 different elevations based on FLEX<sup>+</sup> model.

929 **5.5**

930 **6.3 Runoff generation mechanisms at different elevation**  
 931 **zones/elevations and across landscapes**

932 Elevation is a key topographic factor influencing basin fundamental control on runoff  
 933 processes/generation and their seasonal hydrological variability in mountainous basins,

934 as it affects governs precipitation patterns phase, snow storage accumulation, and melt  
935 rate timing (Jenicek and Ledvinka, 2020)(Jenicek and Ledvinka, 2020). In the study  
936 basins, runoff contributions increase progressively with elevation. This pattern  
937 contrasts with glacierized catchments, where the largest runoff contributions do not  
938 necessarily originate from the highest elevation bands but are often dominated by  
939 glacier melt processes (Gao et al., 2020). These elevation-dependent contrasts highlight  
940 the importance of explicitly accounting for vertical heterogeneity and basin-specific  
941 cryospheric conditions in cold-region hydrological modelling.

942  
943 The lag effect in Fig.13 shows significant differences in runoff contributions across 5  
944 equal area elevation bands. High elevation areas (above 2900 m or 2825 m) play a  
945 dominant role in runoff generation, primarily due to the orographic effect, which leads  
946 to increased precipitation and a higher proportion of snowmelt contributions (Ayala et  
947 al., 2023) (Fig.12). Runoff peaks in these high elevation areas are especially  
948 pronounced in spring and summer, highlighting the critical role of seasonal  
949 snowmelt. snowmelt runoff across different elevations is a defining feature of  
950 hydrological processes in mountainous basins, arising from the temporal variability of  
951 snowmelt among elevation areas. In the Bogd Uliastai and Zavkhan Guulin river basins,  
952 low elevation areas contribute rapidly to runoff during the initial stages, while high  
953 elevation areas gradually augment runoff as the season progresses, reflecting the  
954 delayed response of snowmelt-dominated areas (Hajika et al., 2024). This lag is  
955 primarily governed by elevation-dependent snow accumulation and melt dynamics:  
956 under cold conditions at higher elevations, precipitation is stored as snow, and  
957 meltwater release typically occurs several weeks to a few months later than at lower  
958 elevations, with the lag being most pronounced at the onset of the melt season (Gillan  
959 et al., 2010) (Fig.12).

960  
961 The lag in snowmelt runoff across different elevations has profound implications for  
962 water resources management. Snowmelt from high elevation areas prolongs the  
963 recession of basin runoff, maintaining downstream water supply and providing

964 buffering capacity during droughts or low-flow periods. In contrast, low elevation areas  
965 respond rapidly to extreme precipitation, generating short-term flood peaks, while  
966 delayed high elevation snowmelt can extend high flow conditions, complicating flood  
967 management (Gu et al., 2023). Effective management in mountainous basins therefore  
968 requires integrating both immediate and delayed runoff contributions across elevations  
969 to optimize water allocation, improve flood early-warning accuracy, and safeguard  
970 downstream ecological and socio-economic water demands (Li et al., 2019).

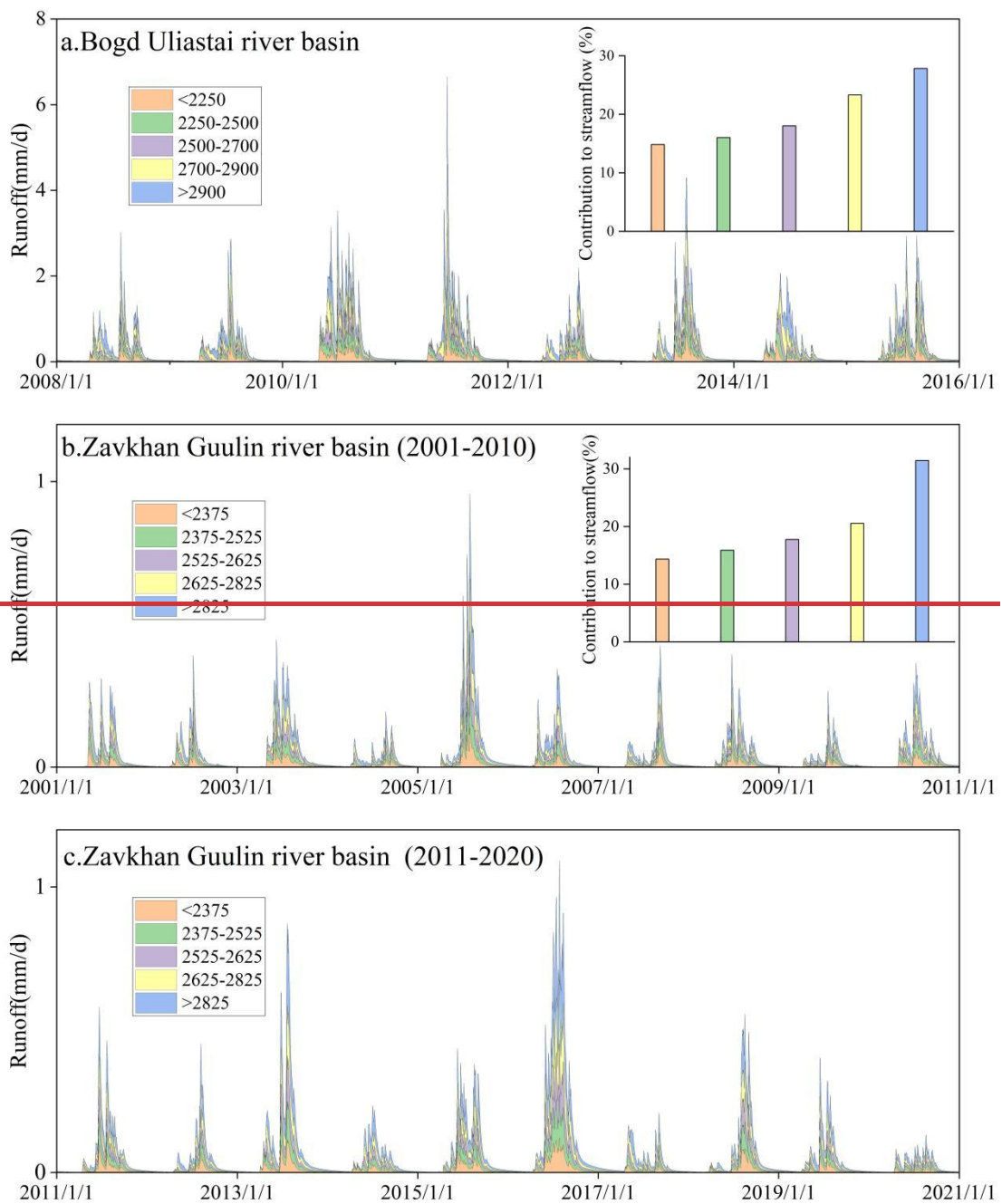
971  
972 Beyond elevation controls, vegetation influences runoff generation through its direct  
973 physiological properties (e.g., interception and root zone storage). Grasslands are the  
974 dominant land-cover type in both basins and are widely distributed across different  
975 elevation zones. Their runoff-generation characteristics are relatively spatially uniform  
976 in a basin-averaged sense and thus exert a primary control on the overall runoff response.  
977 Under the semi-arid and arid climatic setting, soils in grassland areas are generally  
978 persistently dry, with a large initial soil-moisture deficit. This condition thereby  
979 enhances the infiltration demand for rainfall and snowmelt, delaying runoff generation  
980 (Xue et al., 2025). Forested areas exhibit strong regulatory functions—intercepting  
981 precipitation, enhancing infiltration, and reducing quick flow generation (Liu et al.,  
982 2018; Stocker et al., 2023). Riparian areas function as hydrologically connected source  
983 areas, rapidly transmitting rainfall and snowmelt to the channel network —In contrast,  
984 low elevation areas rely primarily on rainfall-induced runoff. Due to limited  
985 precipitation and higher evaporative losses, their contributions to total runoff are  
986 comparatively smaller (Sprenger et al., 2022).

987  
988 The lag effect in runoff is a notable characteristic of hydrological processes in  
989 mountainous basins, reflecting the differential responses of various elevation areas to  
990 hydrological drivers. In the Bogd Uliastai river basin, low elevation areas respond  
991 rapidly to precipitation events, contributing significantly to runoff during the early  
992 stages of peak flow. As the event progresses, contributions from higher elevation areas

993 gradually increase, highlighting the heterogeneous influence of elevation on runoff  
994 dynamics (Hajika et al., 2024). This lag is closely associated with delayed snowmelt  
995 process in high elevation areas, where lower temperatures cause precipitation to fall as  
996 snow. Snowmelt in these areas typically occurs weeks or even months later than in  
997 lower elevations, with the delay especially evident during the initial stages of the melt  
998 season (Gillan et al., 2010). A similar pattern is observed in the Zavkhan-Guulin river  
999 basin, where runoff from high elevation continues to contribute significantly during the  
1000 latter part of the hydrograph, thereby prolonging the recession phase (Fig.13).

1001  
1002 The lag effect of runoff across different elevation areas has important implications for  
1003 water resource management. In cold, high mountain basins, the delayed hydrological  
1004 response of upper elevation not only sustains downstream water supply during dry  
1005 periods, but also significantly influences the timing and spatial extent of flood risk (Gu  
1006 et al., 2023). During extreme precipitation events, rapid runoff generation in low-  
1007 elevation areas may exacerbate short-term flood hazards, while delayed snowmelt from  
1008 higher elevations can prolong flood durations. Therefore, both immediate and delayed  
1009 hydrological responses should be holistically considered in catchment-scale  
1010 management strategies (Li et al., 2019).

1011  
1012 Although the lag effect is particularly evident during runoff peaks, current observational  
1013 and modeling data remain insufficient to accurately quantify the specific response  
1014 timings and processes across elevation gradients. Future research should integrate high-  
1015 resolution numerical simulations with field-based observations to better disentangle the  
1016 dynamic runoff contributions from different elevation areas, thereby enhancing the  
1017 predictive skill and physical realism of hydrological models.



1018

1019 **Fig.13** Runoff contribution from 5 equal area elevation bands (each representing 20% of the total  
 1020 catchment area) based on FLEX<sup>+</sup> model.

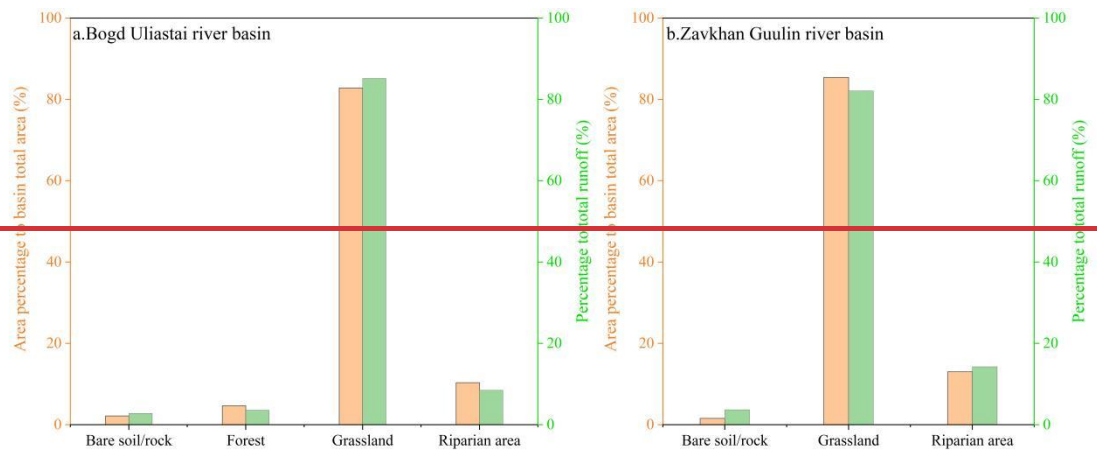
1021

1022 **5.6 Regulatory mechanisms of vegetation in runoff generation**  
 1023 **processes**

1024 ~~Vegetation influences runoff generation not only through its direct physiological~~  
 1025 ~~properties (e.g., interception, root zone storage, and transpiration), but also through its~~

1026 spatial interactions with topography. To examine this regulatory role, we analyzed  
1027 runoff responses across HRUs delineated by distinct vegetation types and elevation  
1028 bands, thereby isolating process-driven variability from effects primarily driven by  
1029 areal extent (Fig.14).

1030 Despite grasslands occupying the largest portion of both basins (82.8% and 85.4%),  
1031 their runoff generation capacity varies markedly with elevation and climatic context. In  
1032 the more arid Zavkhan Guulin river basin, dry grassland soils exhibit high infiltration  
1033 rates under unsaturated conditions, thereby reducing surface runoff. However, during  
1034 peak melt or rainfall events, saturation thresholds are exceeded, triggering rapid surface  
1035 runoff (Assouline et al., 2024).



1036 **Fig.14** Runoff contribution from different landscapes based on FLEX<sup>T</sup> model.

1037  
1038  
1039 Riparian zones, although limited in area (10.3% and 13.0%), contribute  
1040 disproportionately to runoff (8.5% and 14.2%) due to high soil moisture, shallow root  
1041 zones, and strong hydrological connectivity. This is consistent with findings that  
1042 riparian areas function as dynamic runoff buffers, responding rapidly to precipitation  
1043 and snowmelt inputs (Leibowitz et al., 2023)(Leibowitz et al., 2023).

1044  
1045 Forested areas, found only in the Bogd Uliastai basin, exhibit strong regulatory  
1046 functions—intercepting precipitation, enhancing infiltration, and reducing quick flow  
1047 generation (Liu et al., 2018; Stocker et al., 2023). These effects are particularly relevant  
1048 under scenarios of climate-induced vegetation change.

1049

1050 ~~The runoff generation capacity of bare soil/rock is high due to the lack of vegetation and~~  
1051 ~~low soil permeability. After rainfall or snowmelt, water infiltrates poorly and rapidly~~  
1052 ~~forms overland flow (Zeng et al., 2024). However, bare surfaces cover only a small~~  
1053 ~~portion of the catchment (2.2% and 1.6%), so their overall contribution to streamflow~~  
1054 ~~remains limited (2.8% and 3.7%). Despite their distinct hydrological behavior, bare~~  
1055 ~~areas play a secondary but notable role in runoff dynamics.~~

1056  
1057 ~~Importantly, our simulations reveal that interactions between vegetation and~~  
1058 ~~topography play a critical role in shaping runoff dynamics. At higher elevations, where~~  
1059 ~~vegetation is sparse and terrain is steep, snowmelt is rapidly converted into surface~~  
1060 ~~runoff due to limited soil storage capacity. In contrast, lower elevation areas dominated~~  
1061 ~~by grasslands and wetlands benefit from gentler slopes and deeper root zones, which~~  
1062 ~~enhance infiltration and delay runoff responses (Caviedes-Voullième et al., 2021).~~

1063  
1064 . The runoff generation capacity of bare soil/rock is high due to the lack of vegetation  
1065 and low soil permeability. After rainfall or snowmelt, water infiltrates poorly and  
1066 rapidly forms overland flow (Zeng et al., 2024). Although their basin-scale contribution  
1067 is constrained by areal extent, these surfaces can locally intensify runoff responses and  
1068 sediment transport.

1069  
1070 These findings support the view that vegetation functions as a spatially variable  
1071 regulator of runoff generation, ~~contingent on topographic context and soil-plant-~~  
1072 ~~atmosphere interactions.~~ This regulatory effect is particularly sensitive to future  
1073 changes in vegetation cover and distribution under climate and land use change  
1074 scenarios. For instance, overgrazing may reduce aboveground biomass and root zone  
1075 storage capacity, thereby increasing runoff and erosion risks (Donovan and Monaghan,  
1076 2021)(Donovan and Monaghan, 2021); while shifts in vegetation type (e.g., shrub  
1077 encroachment or forest decline) could alter hydrological partitioning along elevation  
1078 gradients (Hsu et al., 2025; Zhou et al., 2023)(Hsu et al., 2025; Zhou et al., 2023).

1079

## 1080 **6.4 Applicability and limitations of the modelling framework**

1081 Previous applications of the FLEX framework in alpine basins, such as the Heihe river  
1082 basin, provide an important reference for interpreting the results of this study. In the  
1083 Heihe river basin, FLEX<sup>T</sup> was configured using terrain-driven functional units,  
1084 whereby the catchment was discretized into four topographic sub-units representing  
1085 distinct dominant hydrological processes. This modelling strategy primarily focused on  
1086 assessing model realism and transferability across sub-basins by demonstrating the  
1087 ability of FLEX<sup>T</sup> to reproduce contrasting functional hydrological behaviors (Gao et al.,  
1088 2014). Building on these earlier studies, the present work further demonstrates that the  
1089 FLEX framework can also be adapted to colder and more semi-arid conditions using a  
1090 stepwise strategy. Importantly, our emphasis extends beyond discharge performance to  
1091 diagnosing runoff-generation mechanisms—specifically the snowmelt contribution to  
1092 streamflow and the relative roles of elevation bands and vegetation units—thereby  
1093 clarifying how topography and land cover jointly shape hydrological responses in cold  
1094 alpine basins.

1095

1096 While the proposed modelling framework captures key hydrological processes, several  
1097 limitations should be acknowledged. First, frozen soil processes were not explicitly  
1098 represented in this study due to data constraints. Frozen soil is widespread across the  
1099 region and can exert strong controls on hydrological processes by restricting moisture  
1100 exchange between deeper soil layers and the atmosphere, reducing soil permeability,  
1101 and modifying near-surface flow pathways (Li et al., 2025). These effects may influence  
1102 the partitioning between surface runoff and subsurface flow, particularly in high-  
1103 elevation permafrost regions with sparse vegetation (Hu et al., 2025). In this study, the  
1104 elevation-dependent runoff generation patterns identified may partly reflect the  
1105 integrated influence of frozen soil conditions in these regions. Future studies that  
1106 explicitly incorporate frozen soil dynamics would help to further disentangle the  
1107 interacting roles of topography, vegetation, and frozen ground in shaping hydrological

1108 responses in alpine basins.

1109  
1110 Second, regarding the assumption of complete mixing in snowmelt runoff tracking, the  
1111 applied conceptual model represents storages as lumped and homogeneous reservoirs,  
1112 within which incoming rainfall and snowmelt are assumed to mix instantaneously with  
1113 pre-event water. Despite its limited ability to explicitly represent rapid snowmelt runoff  
1114 responses and flow-path heterogeneity at the event scale (Weiler et al., 2018), this  
1115 assumption is still widely applied in catchment-scale estimates of snowmelt runoff  
1116 contributions and is regarded as robust at long time scales (Li et al., 2017; Liu et al.,  
1117 2023; Wu et al., 2021). Importantly, the snowmelt tracker is designed to estimate the  
1118 long-term average of the fraction of total streamflow that originates from snowmelt,  
1119 rather than event-scale responses.

1120  
1121 Finally, the use of two study basins entails both advantages and limitations. Focusing  
1122 on a limited number of basins allows for detailed process interpretation and reduces  
1123 confounding effects associated with excessive climatic or physiographic diversity, but  
1124 it also constrains the generalization of the findings (Hrachowitz et al., 2013). The  
1125 identified runoff generation mechanisms and model performance characteristics should  
1126 therefore be interpreted as representative of cold, semi-arid alpine basins with similar  
1127 hydroclimatic and geomorphic settings, rather than as universally applicable.  
1128 Expanding the analysis to a larger set of basins would be necessary to assess model  
1129 robustness and transferability more rigorously.

## 1131 7. Conclusions

1132 Hydrological modelling in cold and high-latitude regions ~~poses considerable~~remains  
1133 challenges due to ~~the complexity of complex~~ cryospheric processes and limited  
1134 observational data. To address these issues, this study ~~proposes~~developed and tested a  
1135 stepwise modelling framework that ~~incrementally refines model structures by~~  
1136 ~~incorporating progressively incorporates~~ key hydrological processes and landscape

1137 characteristics, ~~thereby enhancing both the physical realism and with the aim of~~  
1138 ~~improving both~~ predictive performance ~~of the model and process interpretability.~~

1139  
1140 ~~Our~~The results ~~underscore the limitations of the~~demonstrate that model structure  
1141 ~~matters. The~~ lumped models (FLEX<sup>L</sup> and FLEX<sup>L-S</sup>) ~~in accurately representing are~~  
1142 ~~insufficient for capturing~~ runoff dynamics, ~~particularly in regions~~basins with complex  
1143 topography and heterogeneous vegetation ~~cover~~. Although ~~the distributed model~~  
1144 FLEX<sup>D</sup> ~~improved the~~improves simulation ~~of runoff variability by incorporating by~~  
1145 ~~using~~ spatially distributed inputs, it still lacks full physical interpretability ~~of its~~  
1146 ~~parameters~~. In contrast, the landscape-based FLEX<sup>T</sup> model ~~explicitly~~ integrates  
1147 snowpack, topography, and vegetation characteristics, ~~thereby enhancing the~~providing  
1148 ~~more~~ physical ~~realism of meaningful~~ parameterization and ~~offering~~a more mechanistic  
1149 representation of hydrological processes. ~~While FLEX<sup>T</sup> achieved performance~~  
1150 ~~comparable to FLEX<sup>D</sup> in simulating catchment runoff dynamics, this outcome may be~~  
1151 ~~attributed to the limited vegetation heterogeneity in the study basins. Nonetheless,~~  
1152 ~~validation~~Validation using SWE ~~confirmed~~further confirms the FLEX<sup>T</sup>'s  
1153 ~~capability~~ability to capture seasonal ~~patterns~~dynamics, interannual variability, and key  
1154 hydrological mechanisms in cryospheric environments. These findings underscore the  
1155 potential advantages of FLEX<sup>T</sup>, particularly in basins with greater ecological or  
1156 topographic complexity.

1157  
1158 Results from the FLEX<sup>T</sup> model indicate that snowmelt ~~contributes~~runoff accounts for  
1159 ~~23.56%±0.7% and 15.9%±1.3% and 14.7%±1.6% to~~of streamflow in the Bogd Uliastai  
1160 and Zavkhan Guulin river basins, respectively. ~~Temporally, snowmelt contributions~~  
1161 ~~peak in~~Snowmelt runoff dominates streamflow during spring and ~~remain minimal~~  
1162 ~~during other seasons. Spatially, snowmelt contributions increase~~increases with  
1163 elevation, underscoring the critical role of topography in shaping ~~the spatiotemporal~~  
1164 ~~dynamics of~~ runoff generation. In high elevation areas, the lagged snowmelt response  
1165 leads to a sustained and gradual release of runoff, whereas low ~~altitude~~ elevation areas  
1166 ~~respond more rapidly to~~ dominated by rainfall ~~events. Moreover, hydrological~~

~~modelling approaches based on vegetation landscape classifications better capture spatial heterogeneity and characterize the generate rapid runoff. Controlled by distinct dominant hydrological mechanisms across, different landscape units contribute unequally to streamflow.~~

These findings offer valuable insights into hydrological response mechanisms in cold alpine basins ~~with limited observational data~~ on the Mongolian Plateau. The stepwise ~~modeling~~ modelling framework ~~developed in this study not only improves the simulation of runoff dynamics in high-latitude regions but also enhances understanding of model realism in~~ cryospheric hydrological responses to global climate change. ~~Importantly, this framework holds both scientific environments and provides practical value, providing a foundation for more effective~~ support for water resource management, ecological conservation, and climate adaptation in ~~eryospheric high-latitude~~ and data-scarce regions.

#### **Code availability**

The code is available upon request to the contact author.

#### **Data availability**

All data presented in this manuscript are publicly available for download from: Hydrometeorological data (precipitation, runoff, temperature) from the Information and Research Institute of Meteorology, Hydrology, and Environment, available at ~~http://irimhe.namem.gov.mn~~<http://irimhe.namem.gov.mn>. Arctic Snow Water Equivalent Grid Dataset from the National Tibetan Plateau/Third Pole Environment Data Center, available at ~~https://estr.cn/18406.11.Snow.tpdc.271556~~<https://estr.cn/18406.11.Snow.tpdc.271556>. Shuttle Radar Topography Mission Digital Elevation Model (SRTM-DEM), available at ~~http://srtm.csi.cgiar.org~~<http://srtm.csi.cgiar.org>. Sentinel-2 10-meter Land Use/Land Cover data from the ESRI Living Atlas, available at ~~https://livingatlas.arcgis.com/landcover/~~<https://livingatlas.arcgis.com/landcover/>.

1197 NDVI data were obtained from the United States Geological Survey (USGS)  
1198 EarthExplorer platform. available at  
1199 <https://earthexplorer.usgs.gov/><https://earthexplorer.usgs.gov/>.

1200

### 1201 **Author contributions**

1202 LY and HG designed the study. BD provided the valuable fieldwork data. LY, YW, HG,  
1203 and ZD conducted the analyses. LY wrote the paper. All authors discussed the results  
1204 and the first draft and contributed to the final paper.

1205

### 1206 **Acknowledgments**

1207 This research is funded by National Key Research and Development Program of China.  
1208 (2024YFE0113200), the National Natural Science Foundation of China (grant no.  
1209 42471040). Zheng Duan would like to acknowledge the support from the Crafoord  
1210 Foundation, Sweden (Grant No.20210552 and No.20240857). This work was  
1211 performed as part of the IAHS HELPING Working Group on "Development &  
1212 application of river basin simulators".

1213

### 1214 **References**

- 1215 ~~Antonelli, A. et al., 2018. Geological and climatic influences on mountain biodiversity. Nature~~  
1216 ~~Geoscience, 11(10): 718–725. DOI:10.1038/s41561-018-0236-z~~  
1217 ~~Assouline, S., Sela, S., Dorman, M., Svoray, T., 2024. Runoff generation in a semiarid environment: The~~  
1218 ~~role of rainstorm intra-event temporal variability and antecedent soil moisture. Advances in~~  
1219 ~~Water Resources, 188: 104715. DOI:https://doi.org/10.1016/j.advwatres.2024.104715~~  
1220 ~~Ayala, Á., Schauwecker, S., MacDonell, S., 2023. Spatial distribution and controls of snowmelt runoff~~  
1221 ~~in a sublimation-dominated environment in the semiarid Andes of Chile. Hydrol. Earth Syst.~~  
1222 ~~Sci., 27(18): 3463–3484. DOI:10.5194/hess-27-3463-2023~~  
1223 ~~Baasanmunkh, S. et al., 2019. Contribution to the knowledge on the flora of northern Mongolia. Journal~~  
1224 ~~of Asia-Pacific Biodiversity, 12(4): 643–660. DOI:https://doi.org/10.1016/j.japb.2019.08.009~~  
1225 ~~Barnett, T.P., Adam, J.C., Lettenmaier, D.P., 2005. Potential impacts of a warming climate on water~~  
1226 ~~availability in snow-dominated regions. Nature, 438(7066): 303–309.~~  
1227 ~~DOI:10.1038/nature04141~~  
1228 ~~Beven, K.J., 2012. Rainfall runoff modeling: the primer. Rainfall runoff modelling: the primer, 15(1):~~  
1229 ~~84–96.~~  
1230 ~~Bormann, H., Breuer, L., Giertz, S., Huisman, J.A., Viney, N.R., 2009. Spatially explicit versus lumped~~  
1231 ~~models in catchment hydrology—experiences from two case studies. In: Baveye, P.C., Laba,~~

1232 M., Mysiak, J. (Eds.), *Uncertainties in Environmental Modelling and Consequences for Policy*  
1233 *Making*. Springer Netherlands, Dordrecht, pp. 3–26.—

1234 Broxton, P.D., van Leeuwen, W.J.D., Biederman, J.A., 2020. Forest cover and topography regulate the  
1235 thin, ephemeral snowpacks of the semiarid Southwest United States. *Ecohydrology*, 13(4):  
1236 e2202. DOI:<https://doi.org/10.1002/eco.2202>

1237 Caviedes-Voullième, D., Ahmadiya, E., Hinz, C., 2021. Interactions of Microtopography, Slope and  
1238 Infiltration Cause Complex Rainfall-Runoff Behavior at the Hillslope Scale for Single Rainfall  
1239 Events. *WATER RESOURCES RESEARCH*, 57(7). DOI:10.1029/2020WR028127

1240 Chen, J. et al., 2023. Differences in soil water storage, consumption, and use efficiency of typical  
1241 vegetation types and their responses to precipitation in the Loess Plateau, China. *Science of The*  
1242 *Total Environment*, 869: 161710. DOI:<https://doi.org/10.1016/j.scitotenv.2023.161710>

1243 Chen, Y., Li, W., Fang, G., Li, Z., 2017. Review article: Hydrological modeling in glacierized catchments  
1244 of central Asia—status and challenges. *Hydrol. Earth Syst. Sci.*, 21(2): 669–684.  
1245 DOI:10.5194/hess-21-669-2017

1246 Cheng, X., Bai, Y., Zhu, J., Han, H., 2020. Effects of forest thinning on interception and surface runoff  
1247 in *Larix principis rupprechtii* plantation during the growing season. *Journal of Arid*  
1248 *Environments*, 181: 104222. DOI:<https://doi.org/10.1016/j.jaridenv.2020.104222>

1249 Dharmadasa, V., Kinnard, C., Baraër, M., 2023. Topographic and vegetation controls of the spatial  
1250 distribution of snow depth in agro-forested environments by UAV lidar. *The Cryosphere*, 17(3):  
1251 1225–1246. DOI:10.5194/te-17-1225-2023

1252 Donovan, M., Monaghan, R., 2021. Impacts of grazing on ground cover, soil physical properties and soil  
1253 loss via surface erosion: A novel geospatial modelling approach. *Journal of Environmental*  
1254 *Management*, 287: 112206. DOI:<https://doi.org/10.1016/j.jenvman.2021.112206>

1255 Dorjsuren, B. et al., 2024. Trend analysis of hydro-climatic variables in the Great Lakes Depression  
1256 region of Mongolia. *Journal of Water and Climate Change*, 15(3): 940–957.  
1257 DOI:10.2166/wcc.2024.379

1258 Dorjsuren, B. et al., 2023. Hydro-Climatic and Vegetation Dynamics Spatial-Temporal Changes in the  
1259 Great Lakes Depression Region of Mongolia. *Water*. DOI:10.3390/w15213748

1260 Duethmann, D., Peters, J., Blume, T., Vorogushyn, S., Güntner, A., 2014. The value of satellite-derived  
1261 snow cover images for calibrating a hydrological model in snow-dominated catchments in  
1262 Central Asia. *Water Resources Research*, 50(3): 2002–2021.  
1263 DOI:<https://doi.org/10.1002/2013WR014382>

1264 Dwarakish, G.S., Ganasri, B.P., 2015. Impact of land use change on hydrological systems: A review of  
1265 current modeling approaches. *Cogent Geoscience*, 1(1): 1115691.  
1266 DOI:10.1080/23312041.2015.1115691

1267 Fenicia, F., Kavetski, D., Savenije, H.H.G., Pfister, L., 2016. From spatially variable streamflow to  
1268 distributed hydrological models: Analysis of key modeling decisions. *Water Resources*  
1269 *Research*, 52(2): 954–989. DOI:<https://doi.org/10.1002/2015WR017398>

1270 Fenicia, F., McDonnell, J.J., Savenije, H.H.G., 2008a. Learning from model improvement: On the  
1271 contribution of complementary data to process understanding. *Water Resources Research*, 44(6):  
1272 DOI:<https://doi.org/10.1029/2007WR006386>

1273 Fenicia, F., Savenije, H.H.G., Matgen, P., Pfister, L., 2008b. Understanding catchment behavior through  
1274 stepwise model concept improvement. *Water Resources Research*, 44(1):  
1275 DOI:<https://doi.org/10.1029/2006WR005563>

1276 Gao, H., Ding, Y., Zhao, Q., Hrachowitz, M., Savenije, H.H.G., 2017. The importance of aspect for  
1277 modelling the hydrological response in a glacier catchment in Central Asia. *Hydrological*  
1278 *Processes*, 31(16): 2842–2859. DOI:<https://doi.org/10.1002/hyp.11224>

1279 Gao, H., Hrachowitz, M., Fenicia, F., Gharari, S., Savenije, H.H.G., 2014. Testing the realism of a  
1280 topography driven model (FLEX Topo) in the nested catchments of the Upper Heihe, China.  
1281 *Hydrol. Earth Syst. Sci.*, 18(5): 1895–1915. DOI:[10.5194/hess-18-1895-2014](https://doi.org/10.5194/hess-18-1895-2014)

1282 Gillan, B.J., Harper, J.T., Moore, J.N., 2010. Timing of present and future snowmelt from high elevations  
1283 in northwest Montana. *Water Resources Research*, 46(1).  
1284 DOI:<https://doi.org/10.1029/2009WR007861>

1285 Gomes, M.N. et al., 2023. HydroPol2D—Distributed hydrodynamic and water quality model:  
1286 Challenges and opportunities in poorly gauged catchments. *Journal of Hydrology*, 625: 129982.  
1287 DOI:<https://doi.org/10.1016/j.jhydrol.2023.129982>

1288 Greco, R., Marino, P., Bogaard, T.A., 2023. Recent advancements of landslide hydrology. *WILEY*  
1289 *INTERDISCIPLINARY REVIEWS WATER*, 10(6). DOI:[10.1002/wat2.1675](https://doi.org/10.1002/wat2.1675)

1290 Gu, H. et al., 2023. Seasonal catchment memory of high mountain rivers in the Tibetan Plateau. *Nature*  
1291 *Communications*, 14(1): 3173. DOI:[10.1038/s41467-023-38966-9](https://doi.org/10.1038/s41467-023-38966-9)

1292 Gupta, H.V., Kling, H., Yilmaz, K.K., Martinez, G.F., 2009. Decomposition of the mean squared error  
1293 and NSE performance criteria: Implications for improving hydrological modelling. *Journal of*  
1294 *Hydrology*, 377(1): 80–91. DOI:<https://doi.org/10.1016/j.jhydrol.2009.08.003>

1295 Hajika, T., Yamakawa, Y., Uchida, T., 2024. Spatial distribution of rainfall runoff characteristics and  
1296 peak lag time in high relief meso-scale mountain catchments where observations are scarce.  
1297 *Hydrological Processes*, 38(6): e15177. DOI:<https://doi.org/10.1002/hyp.15177>

1298 Hammond, J.C., Harpold, A.A., Weiss, S., Kampf, S.K., 2019. Partitioning snowmelt and rainfall in the  
1299 critical zone: effects of climate type and soil properties. *Hydrol. Earth Syst. Sci.*, 23(9): 3553–  
1300 3570. DOI:[10.5194/hess-23-3553-2019](https://doi.org/10.5194/hess-23-3553-2019)

1301 He, S. et al., 2024. Impacts of re-vegetation on soil water dynamics in a semiarid region of Northwest  
1302 China. *Science of The Total Environment*, 911: 168496.  
1303 DOI:<https://doi.org/10.1016/j.scitotenv.2023.168496>

1304 Hsu, J. et al., 2025. Impact of land-use changes and global warming on extreme precipitation patterns in  
1305 the Maritime Continent. *npj Climate and Atmospheric Science*, 8(1): 5. DOI:[10.1038/s41612-](https://doi.org/10.1038/s41612-024-00883-z)  
1306 [024-00883-z](https://doi.org/10.1038/s41612-024-00883-z)

1307 Immerzeel, W.W., van Beek, L.P.H., Bierkens, M.F.P., 2010. Climate Change Will Affect the Asian Water  
1308 Towers. *Science*, 328(5984): 1382–1385. DOI:[10.1126/science.1183188](https://doi.org/10.1126/science.1183188)

1309 Jenicek, M., Ledvinka, O., 2020. Importance of snowmelt contribution to seasonal runoff and summer  
1310 low flows in Czechia. *Hydrol. Earth Syst. Sci.*, 24(7): 3475–3491. DOI:[10.5194/hess-24-3475-](https://doi.org/10.5194/hess-24-3475-2020)  
1311 [2020](https://doi.org/10.5194/hess-24-3475-2020)

1312 Jiao, Y. et al., 2017. Impact of vegetation dynamics on hydrological processes in a semi arid basin by  
1313 using a land surface hydrology coupled model. *Journal of Hydrology*, 551: 116–131.  
1314 DOI:<https://doi.org/10.1016/j.jhydrol.2017.05.060>

1315 Klemeš, V., 1983. Conceptualization and scale in hydrology. *Journal of Hydrology*, 65(1): 1–23.  
1316 DOI:[https://doi.org/10.1016/0022-1694\(83\)90208-1](https://doi.org/10.1016/0022-1694(83)90208-1)

1317 Klemeš, V., 1989. The modelling of mountain hydrology : the ultimate challenge. IAHS AISH  
1318 publication, 190: 29–43.

1319 Kraaijenbrink, P.D.A., Stigter, E.E., Yao, T., Immerzeel, W.W., 2021. Climate change decisive for Asia's

1320 snow-meltwater supply. *Nature Climate Change*, 11(7): 591-597. DOI:10.1038/s41558-021-  
1321 01074-x

1322 Leibowitz, S.G. et al., 2023. National hydrologic connectivity classification links wetlands with stream  
1323 water quality. *Nature Water*, 1(4): 370-380. DOI:10.1038/s44221-023-00057-w

1324 Li, D., Lettenmaier, D.P., Margulis, S.A., Andreadis, K., 2019. The Role of Rain on Snow in Flooding  
1325 Over the Conterminous United States. *Water Resources Research*, 55(11): 8492-8513.  
1326 DOI:https://doi.org/10.1029/2019WR024950

1327 Li, D., Wrzesien, M.L., Durand, M., Adam, J., Lettenmaier, D.P., 2017. How much runoff originates as  
1328 snow in the western United States, and how will that change in the future? *Geophysical  
1329 Research Letters*, 44(12): 6163-6172. DOI:https://doi.org/10.1002/2017GL073551

1330 Litaor, M.I., Williams, M., Seastedt, T.R., 2008. Topographic controls on snow distribution, soil moisture,  
1331 and species diversity of herbaceous alpine vegetation, Niwot Ridge, Colorado. *Journal of  
1332 Geophysical Research: Biogeosciences*, 113(G2). DOI:https://doi.org/10.1029/2007JG000419

1333 Liu, J., Zhang, Z., Zhang, M., 2018. Impacts of forest structure on precipitation interception and run-off  
1334 generation in a semiarid region in northern China. *Hydrological Processes*, 32(15): 2362-2376.  
1335 DOI:https://doi.org/10.1002/hyp.13156

1336 Liu, Z., Cuo, L., Sun, N., 2023. Tracking snowmelt during hydrological surface processes using a  
1337 distributed hydrological model in a mesoscale basin on the Tibetan Plateau. *Journal of  
1338 Hydrology*, 616: 128796. DOI:https://doi.org/10.1016/j.jhydrol.2022.128796

1339 Lundquist, J.D., Minder, J.R., Neiman, P.J., Sukovich, E., 2010. Relationships between Barrier-Jet  
1340 Heights, Orographic Precipitation Gradients, and Streamflow in the Northern Sierra Nevada.  
1341 *Journal of Hydrometeorology*, 11(5): 1141-1156. DOI:https://doi.org/10.1175/2010JHM1264.1

1342 Luo, Z. et al., 2022. Widespread root zone water bypass for various climates and species: Implications  
1343 for the ecohydrological separation understanding. *Agricultural and Forest Meteorology*, 324:  
1344 109107. DOI:https://doi.org/10.1016/j.agrformet.2022.109107

1345 Nippgen, F., McGlynn, B.L., Marshall, L.A., Emanuel, R.E., 2011. Landscape structure and climate  
1346 influences on hydrologic response. *Water Resources Research*, 47(12).  
1347 DOI:https://doi.org/10.1029/2011WR011161

1348 Oki, T., Kanae, S., 2006. Global Hydrological Cycles and World Water Resources. *Science*, 313(5790):  
1349 1068-1072. DOI:doi:10.1126/science.1128845

1350 Qin, J., Yang, B., Ding, Y., Cui, J., Zhang, Y., 2025. Assessment of runoff generation capacity and total  
1351 runoff contribution for different landscapes in alpine and permafrost watershed. *CATENA*, 249:  
1352 108643. DOI:https://doi.org/10.1016/j.catena.2024.108643

1353 Ragettli, S., Cortés, G., McPhee, J., Pellicciotti, F., 2014. An evaluation of approaches for modelling  
1354 hydrological processes in high elevation, glacierized Andean watersheds. *HYDROLOGICAL  
1355 PROCESSES*, 28(23): 5674-5695. DOI:10.1002/hyp.10055

1356 Roebroek, C.T.J., Melsen, L.A., Hoek van Dijke, A.J., Fan, Y., Teuling, A.J., 2020. Global distribution  
1357 of hydrologic controls on forest growth. *Hydrol. Earth Syst. Sci.*, 24(9): 4625-4639.  
1358 DOI:10.5194/hess-24-4625-2020

1359 Savenije, H.H.G., 2010. HESS Opinions "Topography driven conceptual modelling (FLEX-Topo)".  
1360 *Hydrol. Earth Syst. Sci.*, 14(12): 2681-2692. DOI:10.5194/hess-14-2681-2010

1361 Seibert, J., McDonnell, J.J., 2002. On the dialog between experimentalist and modeler in catchment  
1362 hydrology: Use of soft data for multicriteria model calibration. *Water Resources Research*,  
1363 38(11): 23-1-23-14. DOI:https://doi.org/10.1029/2001WR000978

1364 Sivapalan, M., 2009. The secret to 'doing better hydrological science': change the question!  
1365 Hydrological Processes, 23(9): 1391–1396. DOI:<https://doi.org/10.1002/hyp.7242>

1366 Sivapalan, M., Zhang, L., Vertessy, R., Blöschl, G., 2003. Downward approach to hydrological prediction.  
1367 Hydrological Processes, 17(11): 2099–2099. DOI:<https://doi.org/10.1002/hyp.1426>

1368 Sprenger, M. et al., 2022. Variability of Snow and Rainfall Partitioning Into Evapotranspiration and  
1369 Summer Runoff Across Nine Mountainous Catchments. Geophysical Research Letters, 49(13):  
1370 e2022GL099324. DOI:<https://doi.org/10.1029/2022GL099324>

1371 Sprenger, M. et al., 2024. Stream water sourcing from high elevation snowpack inferred from stable  
1372 isotopes of water: a novel application of  $\delta$  excess values. Hydrol. Earth Syst. Sci., 28(7): 1711–  
1373 1723. DOI:10.5194/hess-28-1711-2024

1374 Stahl, K., Moore, R.D., Floyer, J.A., Asplin, M.G., McKendry, I.G., 2006. Comparison of approaches for  
1375 spatial interpolation of daily air temperature in a large region with complex topography and  
1376 highly variable station density. Agricultural and Forest Meteorology, 139(3): 224–236.  
1377 DOI:<https://doi.org/10.1016/j.agrformet.2006.07.004>

1378 Stephens, C.M., Lall, U., Johnson, F.M., Marshall, L.A., 2021. Landscape changes and their hydrologic  
1379 effects: Interactions and feedbacks across scales. Earth Science Reviews, 212: 103466.  
1380 DOI:<https://doi.org/10.1016/j.earseirev.2020.103466>

1381 Stocker, B.D. et al., 2023. Global patterns of water storage in the rooting zones of vegetation. Nature  
1382 Geoscience, 16(3): 250–256. DOI:10.1038/s41561-023-01125-2

1383 Sun, N. et al., 2022. Forest Canopy Density Effects on Snowpack Across the Climate Gradients of the  
1384 Western United States Mountain Ranges. WATER RESOURCES RESEARCH, 58(1).  
1385 DOI:10.1029/2020WR029194

1386 Tarasova, L., Knoche, M., Dietrich, J., Merz, R., 2016. Effects of input discretization, model complexity,  
1387 and calibration strategy on model performance in a data-scarce glacierized catchment in Central  
1388 Asia. Water Resources Research, 52(6): 4674–4699.  
1389 DOI:<https://doi.org/10.1002/2015WR018551>

1390 Volpe, V., Marani, M., Albertson, J.D., Katul, G., 2013. Root controls on water redistribution and carbon  
1391 uptake in the soil-plant system under current and future climate. Advances in Water Resources,  
1392 60: 110–120. DOI:<https://doi.org/10.1016/j.advwatres.2013.07.008>

1393 Vrugt, J.A., Gupta, H.V., Bouten, W., Sorooshian, S., 2003. A Shuffled Complex Evolution Metropolis  
1394 algorithm for optimization and uncertainty assessment of hydrologic model parameters. Water  
1395 Resources Research, 39(8). DOI:<https://doi.org/10.1029/2002WR001642>

1396 Wang Erlandsson, L. et al., 2016. Global root zone storage capacity from satellite-based evaporation.  
1397 Hydrol. Earth Syst. Sci., 20(4): 1459–1481. DOI:10.5194/hess-20-1459-2016

1398 Wang, G.X. et al., 2021. Critical advances in understanding ecohydrological processes of terrestrial  
1399 vegetation: From leaf to watershed scale. CHINESE SCIENCE BULLETIN-CHINESE, 66(28–  
1400 29): 3667–3683. DOI:10.1360/TB-2020-1339

1401 Wiek, A., Lehmann, P., Hauck, C., Stähli, M., 2023. Impact of topography on in situ soil wetness  
1402 measurements for regional landslide early warning — a case study from the Swiss Alpine  
1403 Foreland. Nat. Hazards Earth Syst. Sci., 23(3): 1059–1077. DOI:10.5194/nhess-23-1059-2023

1404 Wu, X. et al., 2021. Analysis of seasonal snowmelt contribution using a distributed energy balance model  
1405 for a river basin in the Altai Mountains of northwestern China. Hydrological Processes, 35(3):  
1406 e14046. DOI:<https://doi.org/10.1002/hyp.14046>

1407 Xiong, C. et al., 2023. Improved global 250 m 8-day NDVI and EVI products from 2000–2021 using the

1408 [LSTM model. Scientific Data, 10\(1\): 800. DOI:10.1038/s41597-023-02695-x](#)

1409 [Ye, S. et al., 2023. From rainfall to runoff: The role of soil moisture in a mountainous catchment. Journal](#)

1410 [of Hydrology, 625: 130060. DOI:https://doi.org/10.1016/j.jhydrol.2023.130060](#)

1411 [Zeng, X., Peng, X., Liu, T., Dai, Q., Chen, X., 2024. Runoff generation and erosion processes at the rock-](#)

1412 [soil interface of outcrops with a concave surface in a rocky desertification area. CATENA, 239:](#)

1413 [107920. DOI:https://doi.org/10.1016/j.catena.2024.107920](#)

1414 [Zhang, W., Kang, S. e., Shen, Y. p., He, J. q., Chen, A. a., 2017. Response of snow hydrological](#)

1415 [processes to a changing climate during 1961 to 2016 in the headwater of Irtysh River Basin,](#)

1416 [Chinese Altai Mountains. Journal of Mountain Science, 14\(11\): 2295-2310.](#)

1417 [DOI:10.1007/s11629-017-4556-z](#)

1418 [Zhao, R., 1992. The Xinanjiang model applied in China. Journal of Hydrology, 135\(1\): 371-381.](#)

1419 [DOI:https://doi.org/10.1016/0022-1694\(92\)90096-E](#)

1420 [Zhong, X. Y. et al., 2021. Impacts of landscape and climatic factors on snow cover in the Altai Mountains,](#)

1421 [China. Advances in Climate Change Research, 12\(1\): 95-107.](#)

1422 [DOI:https://doi.org/10.1016/j.acere.2021.01.005](#)

1423 [Zhou, S., Yu, B., Lintner, B.R., Findell, K.L., Zhang, Y., 2023. Projected increase in global runoff](#)

1424 [dominated by land surface changes. Nature Climate Change, 13\(5\): 442-449.](#)

1425 [DOI:10.1038/s41558-023-01659-8](#)

1426 [Zhu, G. et al., 2022. Evaporation, infiltration and storage of soil water in different vegetation zones in](#)

1427 [the Qilian Mountains: a stable isotope perspective. Hydrol. Earth Syst. Sci., 26\(14\): 3771-3784.](#)

1428 [DOI:10.5194/hess-26-3771-2022](#)

1429 [Antonelli, A. et al., 2018. Geological and climatic influences on mountain biodiversity. Nature](#)

1430 [Geoscience, 11\(10\): 718-725. DOI:10.1038/s41561-018-0236-z](#)

1431 [Baasanmunkh, S. et al., 2019. Contribution to the knowledge on the flora of northern Mongolia. Journal](#)

1432 [of Asia-Pacific Biodiversity, 12\(4\): 643-660. DOI:https://doi.org/10.1016/j.japb.2019.08.009](#)

1433 [Barnett, T.P., Adam, J.C., Lettenmaier, D.P., 2005. Potential impacts of a warming climate on water](#)

1434 [availability in snow-dominated regions. Nature, 438\(7066\): 303-309.](#)

1435 [DOI:10.1038/nature04141](#)

1436 [Beven, K.J., 2012. Rainfall-runoff modeling :the primer. Rainfall-runoff modelling: the primer, 15\(1\):](#)

1437 [84-96.](#)

1438 [Bormann, H., Breuer, L., Giertz, S., Huisman, J.A., Viney, N.R., 2009. Spatially explicit versus lumped](#)

1439 [models in catchment hydrology – experiences from two case studies. In: Baveye, P.C., Laba,](#)

1440 [M., Mysiak, J. \(Eds.\), Uncertainties in Environmental Modelling and Consequences for Policy](#)

1441 [Making. Springer Netherlands, Dordrecht, pp. 3-26.](#)

1442 [Broxton, P.D., van Leeuwen, W.J.D., Biederman, J.A., 2020. Forest cover and topography regulate the](#)

1443 [thin, ephemeral snowpacks of the semiarid Southwest United States. Ecohydrology, 13\(4\):](#)

1444 [e2202. DOI:https://doi.org/10.1002/ecc.2202](#)

1445 [Chen, J. et al., 2023. Differences in soil water storage, consumption, and use efficiency of typical](#)

1446 [vegetation types and their responses to precipitation in the Loess Plateau, China. Science of The](#)

1447 [Total Environment, 869: 161710. DOI:https://doi.org/10.1016/j.scitotenv.2023.161710](#)

1448 [Cheng, X., Bai, Y., Zhu, J., Han, H., 2020. Effects of forest thinning on interception and surface runoff](#)

1449 [in Larix principis-rupprechtii plantation during the growing season. Journal of Arid](#)

1450 [Environments, 181: 104222. DOI:https://doi.org/10.1016/j.jaridenv.2020.104222](#)

1451 [Dharmadasa, V., Kinnard, C., Baraër, M., 2023. Topographic and vegetation controls of the spatial](#)

1452 [distribution of snow depth in agro-forested environments by UAV lidar. \*The Cryosphere\*, 17\(3\):](#)  
1453 [1225-1246. DOI:10.5194/tc-17-1225-2023](#)

1454 [Donovan, M., Monaghan, R., 2021. Impacts of grazing on ground cover, soil physical properties and soil](#)  
1455 [loss via surface erosion: A novel geospatial modelling approach. \*Journal of Environmental\*](#)  
1456 [Management, 287: 112206. DOI:https://doi.org/10.1016/j.jenvman.2021.112206](#)

1457 [Dorjsuren, B. et al., 2024. Trend analysis of hydro-climatic variables in the Great Lakes Depression](#)  
1458 [region of Mongolia. \*Journal of Water and Climate Change\*, 15\(3\): 940-957.](#)  
1459 [DOI:10.2166/wcc.2024.379](#)

1460 [Dorjsuren, B. et al., 2023. Hydro-Climatic and Vegetation Dynamics Spatial-Temporal Changes in the](#)  
1461 [Great Lakes Depression Region of Mongolia, \*Water\*. DOI:10.3390/w15213748](#)

1462 [Duethmann, D., Peters, J., Blume, T., Vorogushyn, S., Güntner, A., 2014. The value of satellite-derived](#)  
1463 [snow cover images for calibrating a hydrological model in snow-dominated catchments in](#)  
1464 [Central Asia. \*Water Resources Research\*, 50\(3\): 2002-2021.](#)  
1465 [DOI:https://doi.org/10.1002/2013WR014382](#)

1466 [Dwarakish, G.S., Ganasri, B.P., 2015. Impact of land use change on hydrological systems: A review of](#)  
1467 [current modeling approaches. \*Cogent Geoscience\*, 1\(1\): 1115691.](#)  
1468 [DOI:10.1080/23312041.2015.1115691](#)

1469 [Feng, J., Alifujiang, Y., Kozhokulov, S., Jiang, Y., Yang, P., 2025. Quantifying hydrological sensitivity in](#)  
1470 [Central Asia: A multi-factor budyko framework analysis \(2000–2020\). \*Journal of Hydrology:\*](#)  
1471 [Regional Studies, 61: 102746. DOI:https://doi.org/10.1016/j.ejrh.2025.102746](#)

1472 [Fenicia, F., Kavetski, D., Savenije, H.H.G., Pfister, L., 2016. From spatially variable streamflow to](#)  
1473 [distributed hydrological models: Analysis of key modeling decisions. \*Water Resources\*](#)  
1474 [Research, 52\(2\): 954-989. DOI:https://doi.org/10.1002/2015WR017398](#)

1475 [Fenicia, F., McDonnell, J.J., Savenije, H.H.G., 2008a. Learning from model improvement: On the](#)  
1476 [contribution of complementary data to process understanding. \*Water Resources Research\*, 44\(6\).](#)  
1477 [DOI:https://doi.org/10.1029/2007WR006386](#)

1478 [Fenicia, F., Savenije, H.H.G., Matgen, P., Pfister, L., 2008b. Understanding catchment behavior through](#)  
1479 [stepwise model concept improvement. \*Water Resources Research\*, 44\(1\).](#)  
1480 [DOI:https://doi.org/10.1029/2006WR005563](#)

1481 [Gao, H., Ding, Y., Zhao, Q., Hrachowitz, M., Savenije, H.H.G., 2017. The importance of aspect for](#)  
1482 [modelling the hydrological response in a glacier catchment in Central Asia. \*Hydrological\*](#)  
1483 [Processes, 31\(16\): 2842-2859. DOI:https://doi.org/10.1002/hyp.11224](#)

1484 [Gao, H. et al., 2020. Stepwise modeling and the importance of internal variables validation to test model](#)  
1485 [realism in a data scarce glacier basin. \*Journal of Hydrology\*, 591: 125457.](#)  
1486 [DOI:https://doi.org/10.1016/j.jhydrol.2020.125457](#)

1487 [Gao, H., Hrachowitz, M., Fenicia, F., Gharari, S., Savenije, H.H.G., 2014. Testing the realism of a](#)  
1488 [topography-driven model \(FLEX-Topo\) in the nested catchments of the Upper Heihe, China.](#)  
1489 [Hydrol. Earth Syst. Sci., 18\(5\): 1895-1915. DOI:10.5194/hess-18-1895-2014](#)

1490 [Gillan, B.J., Harper, J.T., Moore, J.N., 2010. Timing of present and future snowmelt from high elevations](#)  
1491 [in northwest Montana. \*Water Resources Research\*, 46\(1\).](#)  
1492 [DOI:https://doi.org/10.1029/2009WR007861](#)

1493 [Gomes, M.N. et al., 2023. HydroPol2D — Distributed hydrodynamic and water quality model:](#)  
1494 [Challenges and opportunities in poorly-gauged catchments. \*Journal of Hydrology\*, 625: 129982.](#)  
1495 [DOI:https://doi.org/10.1016/j.jhydrol.2023.129982](#)

1496 [Gu, H. et al., 2023. Seasonal catchment memory of high mountain rivers in the Tibetan Plateau. Nature](#)  
1497 [Communications, 14\(1\): 3173. DOI:10.1038/s41467-023-38966-9](#)

1498 [Gupta, H.V., Kling, H., Yilmaz, K.K., Martinez, G.F., 2009. Decomposition of the mean squared error](#)  
1499 [and NSE performance criteria: Implications for improving hydrological modelling. Journal of](#)  
1500 [Hydrology, 377\(1\): 80-91. DOI:https://doi.org/10.1016/j.jhydrol.2009.08.003](#)

1501 [Hajika, T., Yamakawa, Y., Uchida, T., 2024. Spatial distribution of rainfall–runoff characteristics and](#)  
1502 [peak lag time in high-relief meso-scale mountain catchments where observations are scarce.](#)  
1503 [Hydrological Processes, 38\(6\): e15177. DOI:https://doi.org/10.1002/hyp.15177](#)

1504 [Hammond, J.C., Harpold, A.A., Weiss, S., Kampf, S.K., 2019. Partitioning snowmelt and rainfall in the](#)  
1505 [critical zone: effects of climate type and soil properties. Hydrol. Earth Syst. Sci., 23\(9\): 3553-](#)  
1506 [3570. DOI:10.5194/hess-23-3553-2019](#)

1507 [Hrachowitz, M. et al., 2013. A decade of Predictions in Ungauged Basins \(PUB\)—a review. Hydrological](#)  
1508 [Sciences Journal, 58\(6\): 1198-1255. DOI:10.1080/02626667.2013.803183](#)

1509 [Hsu, J. et al., 2025. Impact of land use changes and global warming on extreme precipitation patterns in](#)  
1510 [the Maritime Continent. npj Climate and Atmospheric Science, 8\(1\): 5. DOI:10.1038/s41612-](#)  
1511 [024-00883-z](#)

1512 [Hu, S. et al., 2025. Groundwater leakage of an endorheic basin with extensive permafrost coverage in](#)  
1513 [the western Mongolian Plateau. Journal of Hydrology, 657: 133175.](#)  
1514 [DOI:https://doi.org/10.1016/j.jhydrol.2025.133175](#)

1515 [Immerzeel, W.W., van Beek, L.P.H., Bierkens, M.F.P., 2010. Climate Change Will Affect the Asian Water](#)  
1516 [Towers. Science, 328\(5984\): 1382-1385. DOI:doi:10.1126/science.1183188](#)

1517 [Jenicek, M., Ledvinka, O., 2020. Importance of snowmelt contribution to seasonal runoff and summer](#)  
1518 [low flows in Czechia. Hydrol. Earth Syst. Sci., 24\(7\): 3475-3491. DOI:10.5194/hess-24-3475-](#)  
1519 [2020](#)

1520 [Jiao, Y. et al., 2017. Impact of vegetation dynamics on hydrological processes in a semi-arid basin by](#)  
1521 [using a land surface-hydrology coupled model. Journal of Hydrology, 551: 116-131.](#)  
1522 [DOI:https://doi.org/10.1016/j.jhydrol.2017.05.060](#)

1523 [Klemeš, V., 1983. Conceptualization and scale in hydrology. Journal of Hydrology, 65\(1\): 1-23.](#)  
1524 [DOI:https://doi.org/10.1016/0022-1694\(83\)90208-1](#)

1525 [Klemeš, V., 1989. The modelling of mountain hydrology : the ultimate challenge. IAHS-AISH](#)  
1526 [publication, 190: 29-43.](#)

1527 [Klimek, K., Starkel, L., 1980. Vertical zonality in the Southern Khangai Mountains \(Mongolia\): result of](#)  
1528 [the polish-mongolian physico-geographical expedition, Vol.I, Geographical studies. Polish](#)  
1529 [Academy of Sciences, Wroclaw.](#)

1530 [Leibowitz, S.G. et al., 2023. National hydrologic connectivity classification links wetlands with stream](#)  
1531 [water quality. Nature Water, 1\(4\): 370-380. DOI:10.1038/s44221-023-00057-w](#)

1532 [Li, D., Lettenmaier, D.P., Margulis, S.A., Andreadis, K., 2019. The Role of Rain-on-Snow in Flooding](#)  
1533 [Over the Conterminous United States. Water Resources Research, 55\(11\): 8492-8513.](#)  
1534 [DOI:https://doi.org/10.1029/2019WR024950](#)

1535 [Li, D., Wrzesien, M.L., Durand, M., Adam, J., Lettenmaier, D.P., 2017. How much runoff originates as](#)  
1536 [snow in the western United States, and how will that change in the future? Geophysical](#)  
1537 [Research Letters, 44\(12\): 6163-6172. DOI:https://doi.org/10.1002/2017GL073551](#)

1538 [Li, F., Wang, J., Li, P., Dashtseren, A., 2025. Review of Permafrost Degradation in the Mongolian Plateau.](#)  
1539 [Land, 14\(2\): 383.](#)

1540 [Liu, J., Zhang, Z., Zhang, M., 2018. Impacts of forest structure on precipitation interception and run-off](#)  
1541 [generation in a semiarid region in northern China. \*Hydrological Processes\*, 32\(15\): 2362-2376.](#)  
1542 [DOI:https://doi.org/10.1002/hyp.13156](#)

1543 [Liu, Z., Cuo, L., Sun, N., 2023. Tracking snowmelt during hydrological surface processes using a](#)  
1544 [distributed hydrological model in a mesoscale basin on the Tibetan Plateau. \*Journal of\*](#)  
1545 [Hydrology, 616: 128796. DOI:https://doi.org/10.1016/j.jhydrol.2022.128796](#)

1546 [Lundquist, J.D., Minder, J.R., Neiman, P.J., Sukovich, E., 2010. Relationships between Barrier Jet](#)  
1547 [Heights, Orographic Precipitation Gradients, and Streamflow in the Northern Sierra Nevada.](#)  
1548 [\*Journal of Hydrometeorology\*, 11\(5\): 1141-1156. DOI:https://doi.org/10.1175/2010JHM1264.1](#)

1549 [Luo, Z. et al., 2022. Widespread root-zone water bypass for various climates and species: Implications](#)  
1550 [for the ecohydrological separation understanding. \*Agricultural and Forest Meteorology\*, 324:](#)  
1551 [109107. DOI:https://doi.org/10.1016/j.agrformet.2022.109107](#)

1552 [Ni, J. et al., 2025. Duration of vegetation green-up response to snowmelt on the Tibetan Plateau.](#)  
1553 [\*Biogeosciences\*, 22\(11\): 2637-2651. DOI:10.5194/bg-22-2637-2025](#)

1554 [Oki, T., Kanae, S., 2006. Global Hydrological Cycles and World Water Resources. \*Science\*, 313\(5790\):](#)  
1555 [1068-1072. DOI:doi:10.1126/science.1128845](#)

1556 [Qin, J., Yang, B., Ding, Y., Cui, J., Zhang, Y., 2025. Assessment of runoff generation capacity and total](#)  
1557 [runoff contribution for different landscapes in alpine and permafrost watershed. \*CATENA\*, 249:](#)  
1558 [108643. DOI:https://doi.org/10.1016/j.catena.2024.108643](#)

1559 [Ragettli, S., Cortés, G., McPhee, J., Pellicciotti, F., 2014. An evaluation of approaches for modelling](#)  
1560 [hydrological processes in high-elevation, glacierized Andean watersheds. \*HYDROLOGICAL\*](#)  
1561 [PROCESSES, 28\(23\): 5674-5695. DOI:10.1002/hyp.10055](#)

1562 [Roebroek, C.T.J., Melsen, L.A., Hoek van Dijke, A.J., Fan, Y., Teuling, A.J., 2020. Global distribution](#)  
1563 [of hydrologic controls on forest growth. \*Hydrol. Earth Syst. Sci.\*, 24\(9\): 4625-4639.](#)  
1564 [DOI:10.5194/hess-24-4625-2020](#)

1565 [Savenije, H.H.G., 2010. HESS Opinions "Topography driven conceptual modelling \(FLEX-Topo\)".](#)  
1566 [\*Hydrol. Earth Syst. Sci.\*, 14\(12\): 2681-2692. DOI:10.5194/hess-14-2681-2010](#)

1567 [Seibert, J., McDonnell, J.J., 2002. On the dialog between experimentalist and modeler in catchment](#)  
1568 [hydrology: Use of soft data for multicriteria model calibration. \*Water Resources Research\*,](#)  
1569 [38\(11\): 23-1-23-14. DOI:https://doi.org/10.1029/2001WR000978](#)

1570 [Sivapalan, M., 2009. The secret to 'doing better hydrological science': change the question!](#)  
1571 [\*Hydrological Processes\*, 23\(9\): 1391-1396. DOI:https://doi.org/10.1002/hyp.7242](#)

1572 [Sivapalan, M., Zhang, L., Vertessy, R., Blöschl, G., 2003. Downward approach to hydrological prediction.](#)  
1573 [\*Hydrological Processes\*, 17\(11\): 2099-2099. DOI:https://doi.org/10.1002/hyp.1426](#)

1574 [Stahl, K., Moore, R.D., Floyer, J.A., Asplin, M.G., McKendry, I.G., 2006. Comparison of approaches for](#)  
1575 [spatial interpolation of daily air temperature in a large region with complex topography and](#)  
1576 [highly variable station density. \*Agricultural and Forest Meteorology\*, 139\(3\): 224-236.](#)  
1577 [DOI:https://doi.org/10.1016/j.agrformet.2006.07.004](#)

1578 [Stephens, C.M., Lall, U., Johnson, F.M., Marshall, L.A., 2021. Landscape changes and their hydrologic](#)  
1579 [effects: Interactions and feedbacks across scales. \*Earth-Science Reviews\*, 212: 103466.](#)  
1580 [DOI:https://doi.org/10.1016/j.earscirev.2020.103466](#)

1581 [Stocker, B.D. et al., 2023. Global patterns of water storage in the rooting zones of vegetation. \*Nature\*](#)  
1582 [Geoscience, 16\(3\): 250-256. DOI:10.1038/s41561-023-01125-2](#)

1583 [Sun, N. et al., 2022. Forest Canopy Density Effects on Snowpack Across the Climate Gradients of the](#)

1584 [Western United States Mountain Ranges. WATER RESOURCES RESEARCH, 58\(1\).](#)  
1585 [DOI:10.1029/2020WR029194](#)

1586 [Tarasova, L., Knoche, M., Dietrich, J., Merz, R., 2016. Effects of input discretization, model complexity,](#)  
1587 [and calibration strategy on model performance in a data-scarce glacierized catchment in Central](#)  
1588 [Asia. Water Resources Research, 52\(6\): 4674-4699.](#)  
1589 [DOI:https://doi.org/10.1002/2015WR018551](#)

1590 [Volpe, V., Marani, M., Albertson, J.D., Katul, G., 2013. Root controls on water redistribution and carbon](#)  
1591 [uptake in the soil–plant system under current and future climate. Advances in Water Resources,](#)  
1592 [60: 110-120. DOI:https://doi.org/10.1016/j.advwatres.2013.07.008](#)

1593 [Vrugt, J.A., Gupta, H.V., Bouten, W., Sorooshian, S., 2003. A Shuffled Complex Evolution Metropolis](#)  
1594 [algorithm for optimization and uncertainty assessment of hydrologic model parameters. Water](#)  
1595 [Resources Research, 39\(8\). DOI:https://doi.org/10.1029/2002WR001642](#)

1596 [Weiler, M., Seibert, J., Stahl, K., 2018. Magic components—why quantifying rain, snowmelt, and icemelt](#)  
1597 [in river discharge is not easy. Hydrological Processes, 32\(1\): 160-166.](#)  
1598 [DOI:https://doi.org/10.1002/hyp.11361](#)

1599 [Wicki, A., Lehmann, P., Hauck, C., Stähli, M., 2023. Impact of topography on in situ soil wetness](#)  
1600 [measurements for regional landslide early warning – a case study from the Swiss Alpine](#)  
1601 [Foreland. Nat. Hazards Earth Syst. Sci., 23\(3\): 1059-1077. DOI:10.5194/nhess-23-1059-2023](#)

1602 [Wu, X. et al., 2021. Analysis of seasonal snowmelt contribution using a distributed energy balance model](#)  
1603 [for a river basin in the Altai Mountains of northwestern China. Hydrological Processes, 35\(3\):](#)  
1604 [e14046. DOI:https://doi.org/10.1002/hyp.14046](#)

1605 [Xiong, C. et al., 2023. Improved global 250 m 8-day NDVI and EVI products from 2000–2021 using the](#)  
1606 [LSTM model. Scientific Data, 10\(1\): 800. DOI:10.1038/s41597-023-02695-x](#)

1607 [Xue, D., Tian, J., Zhang, B., Kang, W., He, C., 2025. Evaluating the effect of vegetation type and](#)  
1608 [topography on infiltration process in an arid mountainous area: Insights from continuous soil](#)  
1609 [moisture monitoring network. Agricultural Water Management, 315: 109537.](#)  
1610 [DOI:https://doi.org/10.1016/j.agwat.2025.109537](#)

1611 [Ye, S. et al., 2023. From rainfall to runoff: The role of soil moisture in a mountainous catchment. Journal](#)  
1612 [of Hydrology, 625: 130060. DOI:https://doi.org/10.1016/j.jhydrol.2023.130060](#)

1613 [Zeng, X., Peng, X., Liu, T., Dai, Q., Chen, X., 2024. Runoff generation and erosion processes at the rock–](#)  
1614 [soil interface of outcrops with a concave surface in a rocky desertification area. CATENA, 239:](#)  
1615 [107920. DOI:https://doi.org/10.1016/j.catena.2024.107920](#)

1616 [Zhang, W., Kang, S.-c., Shen, Y.-p., He, J.-q., Chen, A.-a., 2017. Response of snow hydrological](#)  
1617 [processes to a changing climate during 1961 to 2016 in the headwater of Irtysh River Basin,](#)  
1618 [Chinese Altai Mountains. Journal of Mountain Science, 14\(11\): 2295-2310.](#)  
1619 [DOI:10.1007/s11629-017-4556-z](#)

1620 [Zhao, R., 1992. The Xinanjiang model applied in China. Journal of Hydrology, 135\(1\): 371-381.](#)  
1621 [DOI:https://doi.org/10.1016/0022-1694\(92\)90096-E](#)

1622 [Zhong, X.-Y. et al., 2021. Impacts of landscape and climatic factors on snow cover in the Altai Mountains,](#)  
1623 [China. Advances in Climate Change Research, 12\(1\): 95-107.](#)  
1624 [DOI:https://doi.org/10.1016/j.accre.2021.01.005](#)

1625 [Zhou, S., Yu, B., Lintner, B.R., Findell, K.L., Zhang, Y., 2023. Projected increase in global runoff](#)  
1626 [dominated by land surface changes. Nature Climate Change, 13\(5\): 442-449.](#)  
1627 [DOI:10.1038/s41558-023-01659-8](#)

